



Swansea University
Prifysgol Abertawe



Cronfa - Swansea University Open Access Repository

This is an author produced version of a paper published in :
Journal of Geophysical Research: Atmospheres

Cronfa URL for this paper:

<http://cronfa.swan.ac.uk/Record/cronfa21109>

Paper:

Song, X., Zhang, J., AghaKouchak, A., Roy, S., Xuan, Y., Wang, G., He, R., Wang, X. & Liu, C. (2014). Rapid urbanization and changes in spatiotemporal characteristics of precipitation in Beijing metropolitan area. *Journal of Geophysical Research: Atmospheres*, 119(19), 11,250-11,271.

<http://dx.doi.org/10.1002/2014JD022084>

This article is brought to you by Swansea University. Any person downloading material is agreeing to abide by the terms of the repository licence. Authors are personally responsible for adhering to publisher restrictions or conditions. When uploading content they are required to comply with their publisher agreement and the SHERPA RoMEO database to judge whether or not it is copyright safe to add this version of the paper to this repository.

<http://www.swansea.ac.uk/iss/researchsupport/cronfa-support/>

1 **Rapid urbanization and changes in spatio-temporal characteristics of**
2 **precipitation in Beijing metropolitan area**

3

4 Xiaomeng Song^{1,2}, Jianyun Zhang^{1,2}, Amir AghaKouchak³, Shouraseni Sen Roy⁴, Yunqing Xuan⁵,
5 Guoqing Wang^{1,2}, Ruimin He^{1,2}, Xiaojun Wang^{1,2}, and Cuishan Liu^{1,2}

6

7 ¹State Key Laboratory of Hydrology-Water Resources and Hydraulic Engineering, Nanjing
8 Hydraulic Research Institute, Nanjing, Jiangsu, China

9 ²Research Center for Climate Change, Ministry of Water Resources, Nanjing, Jiangsu, China

10 ³Center for Hydrometeorology and Remote Sensing, University of California, Irvine, Irvine,
11 California, USA

12 ⁴Department of Geography and Regional Studies, University of Miami, Coral Gables, Florida, USA

13 ⁵College of Engineering, Swansea University, Swansea, Wales, UK

14

15 Corresponding author: X. Song, Department of Hydrology and Water Resources, Nanjing Hydraulic
16 Research Institute, Guangzhou Road 225, Gulou District, Nanjing 210029, China
17 (xmsong.cn@gmail.com, xmsong@nhri.cn)

18

19

20 Key Points

- 21 ● Assessed changes in precipitation patterns in Beijing under rapid urbanization
- 22 ● A significantly decreasing trend in annual precipitation is observed
- 23 ● A significant increasing trend in extreme precipitation intensity is observed

24

25 Abstract:

26 This study investigates changes in temporal trends and spatial patterns of precipitation in Beijing
27 over the last six decades. These changes are discussed in the context of rapid urbanization and the
28 growing imbalance between water supply and demand in Beijing. We observed significant decreases
29 in precipitation amounts from 1950 to 2012, with the annual precipitation decreasing by 32% at a
30 decadal rate of 28.5 mm. In particular, precipitation decrease is more pronounced in the summer and
31 warm seasons when water use is at its seasonal peak. We further analyzed hourly precipitation data
32 from 43 rain gauges between 1980 and 2012 to examine the spatio-temporal characteristics of both
33 precipitation amount and intensity across six distinct sub-regions in Beijing. No significant spatial
34 variations in precipitation changes were identified, but slightly greater amounts of precipitation were
35 noted in the urban areas (plains) than in the surrounding suburbs (mountains), due to the effect of
36 urbanization and topography. Precipitation intensity has increased substantially, especially at the
37 hourly duration, as evidenced by the more frequent occurrence of extreme storms. The observed
38 decreased water availability and the increase in extreme weather events require more integrated
39 water management, particularly given the expectation of a warmer and more variable climate, the
40 continued rapid growth of the Beijing metropolis, and the intensifying conflict between water supply
41 and demand.

42 Key words: precipitation pattern, spatio-temporal variation, trend, precipitation intensity, Beijing

43

44 **Index Terms**

45 1854 Precipitation

46 1803 Anthropogenic effects

47 1616 Climate variability

48 1632 Land cover change

49

50 **1. Introduction**

51 Today, more than half of the world's population resides in urban areas, a total projected to reach
52 almost 70% by 2050 [*Li et al.*, 2013; *Seto et al.*, 2011; *United Nations*, 2012]. Along with the rapid
53 population growth, urban expansion also entails artificial changes in land use/cover and decreased
54 albedo [*Han et al.*, 2014a]. These population concentrations are marked by built-up landscapes that
55 transform portions of the Earth's natural surface into impervious surfaces that are rougher in texture
56 and far more heterogeneous than those in surrounding rural areas. Such changes have serious
57 ecological and environmental consequences [*Grimm et al.*, 2008], including deforestation and land
58 fragmentation [*Miller*, 2012], local and regional climate change [*Kaufmann et al.*, 2007], alterations
59 of the hydrological cycle [*Jackson*, 2011; *Ladson et al.*, 2006; *Yang et al.*, 2011], and urban heat
60 islands [*Oke*, 1973], etc. The hydrological impacts of urbanization and heat island formation have
61 been of particular concern [*Chu et al.*, 2013; *Du et al.*, 2012; *Fletcher et al.*, 2013; *Ganeshan et al.*,
62 2013; *Jackson*, 2011]. Specifically, global and regional precipitation changes have been observed for
63 the past few decades across many regions [*Dai*, 2013; *Damberg and AghaKouchak*, 2014; *Hao et al.*,

64 2013; *Yang and Lau, 2004*], especially in urban areas [*Creamean et al., 2013; Pathirana et al., 2014*].
65 Many studies (e.g., the Metropolitan Meteorological Experiment (METROMEX) [*Han et al., 2014a*],
66 the UK Climate Impacts Programme (UKCIP) [*Russell and Hughes, 2012*], and the HYDROMET
67 Integrated Radar Experiment (HIRE'98) [*Berne et al., 2004*]) have examined the effect of
68 urbanization on precipitation, and the consensus view is that the key factors are the urban-rural
69 land-surface discontinuity and the concentration of urban aerosols [*Han and Baik, 2008; Li et al.,*
70 *2011; Pinto et al., 2013; Wang et al., 2012a; Yang et al., 2014*].

71 As one of the world's largest metropolises, Beijing has experienced accelerated urban expansion
72 over the past four decades. The built-up area has increased from 184 km² to 1,350 km² between
73 1973-2012, with the metropolitan population approaching more than 20 million [*Wu, 2012; Yang et*
74 *al., 2014*]. Rapid urbanization introduced myriad new challenges, most notably air quality issues,
75 water scarcity crises, and urban flooding problems. Severe rainstorms and flood events in Beijing
76 have become more frequent in recent years. For instance, the storm event of July 21, 2012 produced
77 a rainfall total in excess of 460 mm in 18 hours, resulting in multiple disasters and 79 casualties
78 [*Zhang et al., 2013a*]. Rapid urbanization also causes the imbalance between water supply and
79 demand to become even more serious. One alarming sign is that aridity and water shortages have
80 become increasingly critical. Recorded observations reveal steadily decreasing precipitation [*Xu et*
81 *al., 2006b; Zhai et al., 2014; Zhu et al., 2012*], especially around the Miyun reservoir area, a primary
82 source for Beijing's water supply [*Zhang et al., 2009*]. In addition, the local effects of declines in
83 precipitation and changes in precipitation pattern – as well as the reasons behind them – have also
84 been of concern in recent years [*Han et al., 2014b; Miao et al., 2009; Sun and Yang, 2008; Wang et*
85 *al., 2009; Zhang et al., 2005; Zhang et al., 2009*]. To some extent, these studies reveal that the local

86 impact factors play an important role in changes in the spatial characteristics and temporal trends of
87 precipitation.

88 There are a large number of studies on Beijing's spatial and temporal variations in precipitation
89 [Xu *et al.*, 2006b; Zhai *et al.*, 2014; Zhang *et al.*, 2009; Zhang *et al.*, 2014; Zhu *et al.*, 2012], changes
90 in precipitation patterns [Li *et al.*, 2008; Wang *et al.*, 2012b; Yin *et al.*, 2011], and the urban effects
91 [Miao *et al.*, 2011; Yang *et al.*, 2014; Zhang *et al.*, 2009]. Li *et al.* [2008] and Wang *et al.* [2012b]
92 showed that both rainfall amount and rainfall frequency present high values from late afternoon to
93 early morning and reach the minima around noon. Zhang *et al.* [2009] investigated the influences of
94 urban expansion on summer heavy precipitation using observations and a mesoscale
95 weather/land-surface/urban-coupled model, and showed that the urban expansion can alter the water
96 vapour conditions and lead to a reduction in precipitation. Miao *et al.* [2011] analyzed the impacts of
97 urbanization on summer precipitation using the Weather Research and Forecasting (WRF) model,
98 and concluded changes in precipitation depends on the degree of urbanization. Most previous studies,
99 however, are limited by the fact that they rely on the data obtained from only a few scattered weather
100 stations focused at the smaller-scale level of meteorological subdivisions and do not address water
101 resource problems caused by changes in precipitation. Even fewer of previous studies have
102 recognized the important role played by topography and urban expansion in the distribution of
103 precipitation, as they can only be well analyzed through the use of more detailed regional subunits
104 and a significantly greater number of rain gauges. This study aims to remedy these shortcomings, and
105 its objectives are to (1) analyze the temporal variations in annual and seasonal precipitation from
106 1950-2012, highlighting the changes in the spatio-temporal characteristics of warm-season
107 (June-September) precipitation across six sub-regions from 1980-2012 within the Beijing area, (2)

108 examine the influence of local factors, especially urbanization and topography on the changes in
109 precipitation, and (3) discuss the water related issues linking the changes in precipitation patterns in
110 Beijing.

111 This paper is organized as follows. The study region, the data and methods are described in
112 Section 2. In Section 3, the temporal variability and spatial distribution of precipitation are discussed,
113 including annual and seasonal precipitation amount, and warm seasonal precipitation intensity.
114 Section 4 explores the possible causes of the observed changes in precipitation patterns. Section 5
115 focuses on implications for water crises in Beijing. Section 6 summarizes the conclusions and
116 remarks.

117

118 **2. Data and methods**

119 2.1 Study area and data sources

120 The Beijing metropolitan area comprises a total area of approximately 16,410 km², of which
121 roughly 38% is relatively flat and 62% is mountainous (Figure 1). The latter is located primarily to
122 the north and west, with elevations averaging 1,000-1,500 m, while the lowland zone lies in the
123 center and southeast, with elevations ranging from 20 to 60 m. Beijing has a monsoon-driven humid
124 continental climate, characterized by hot humid summers and cold dry winters. The mean annual
125 temperature is 11-12°C, and the mean annual precipitation is approximately 600 mm [Zhai *et al.*,
126 2014].

127 In order to effectively analyze the spatial variability of rainfall, the selected stations cover all 16
128 districts in the Beijing metropolitan area, including 14 urban and suburban districts (Dongcheng,
129 Xicheng, Chaoyang, Haidian, Fengtai, Shijingshan, Tongzhou, Shunyi, Changping, Daxing,

130 Mentougou, Fangshan, Pinggu, and Huairou) and two rural counties (Miyun and Yanqing), as shown
131 in Figure 1. To emphasize the important role of terrain in the local distribution of precipitation, *Wang*
132 *et al.* [2012b] suggested to divide Beijing into four zones: urban, suburban, northern mountainous,
133 and southern mountainous areas. Allowing for Beijing's ongoing urban expansion, we follow a
134 similar approach that uses a more detailed matrix of six subregions: the urban area (UA), the inner
135 suburb area in the south (ISAS), the inner suburb area in the north (ISAN), the outer suburb area
136 (OSA), the southwest mountainous area (SWMA), and the northwest mountainous area (NWMA)
137 (see Figure 1). Despite the comparatively large number of rain gauges deployed, only a limited
138 number have long-term records. As such, the information from only those stations that provide
139 precipitation data for at least three decades is collected and analyzed. As a result, the 43 stations
140 meeting these criteria are mapped in Figure 1 and listed in Table 1.

141 [Figure 1 and Table 1 should be inserted here]

142 Monthly and annual mean precipitation data in the Beijing metropolitan area, calculated and
143 provided by the Beijing Hydrological Center of the Beijing Water Authority and based on a network
144 of 16 rain gauges across Beijing, as shown in Figure S1, are used to detect the temporal trend of
145 precipitation between 1950 and 2012. Overall, most of Beijing's precipitation occurs during the
146 warm season (June-September). Therefore, the daily and hourly precipitation data in the warm
147 season from 1980-2012 were collected from 43 stations to analyze the spatial and temporal
148 characteristics of precipitation in Beijing. The density of observations is greatest in the central urban
149 and the surrounding areas, while the coverage of stations in the mountainous zone is relatively sparse.
150 Although some stations were installed as far back as the late 1950s, the observation networks and
151 comprehensive record-keeping did not commence until the 1980s.

152 Annual mean temperature data at Beijing Guanxiangtai weather station (Figure 1) are obtained
153 from the China Meteorological Data Sharing Service System (<http://cdc.cma.gov.cn/home.do>), which
154 is overseen by the Climatic Data Center, National Meteorological Information Center, China
155 Meteorological Administration. Data on urban built-up areas in Beijing are obtained from the Beijing
156 Statistical Annals and China Statistical Yearbook, which is released by the Beijing Statistical Bureau
157 and the State Statistics Bureau and published yearly by China Statistical Press. All water resources
158 data involving the water use and demand data are obtained from the Beijing Water Resources
159 Bulletin and the Beijing Hydrological Regime Annual Report, which is released by the Beijing Water
160 Authority.

161

162 2.2 Methods

163 Four techniques were selected to identify and explain spatio-temporal variations of precipitation
164 in Beijing. First, linear regression and the Mann-Kendall (M-K) test were used to assess the
165 precipitation trends. Second, the spatial distributions of these trends were analyzed by the M-K test
166 and spatial interpolation. Then, the temporal variations were investigated using a moving-average
167 method to cross-check results revealed by the M-K test and linear regression.

168 2.2.1 Linear regression

169 Linear regression is a parametric method used to obtain the slope (or trend) of
170 hydro-meteorological variables over time [*Mosmann et al.*, 2004]. The linear regression equation can
171 be represented as:

$$172 \quad y = a + bx + \varepsilon \quad (1)$$

173 The slope b can be used as an indicator of trend and is calculated as:

174

$$b = \frac{n \sum_{i=1}^n x_i y_i - \sum_{i=1}^n x_i \sum_{i=1}^n y_i}{n \sum_{i=1}^n x_i^2 - \left(\sum_{i=1}^n x_i \right)^2} \quad (2)$$

175 where y_i is a climatic factor, x_i is time, and n is the length of the time sequence. A statistically
176 significant b indicates the slope of a linear trend.

177

178 2.2.2 M-K test

179 The M-K test [*Mann*, 1945; *Kendall*, 1975] is recommended by the World Meteorological
180 Organization (WMO) as a non-parametric method for trend detection because of its robustness and
181 simplicity. The M-K test has been widely used to assess the significance of monotonic trends of
182 hydro-meteorological variables [*Zhang et al.*, 2011, 2012]. For a given time series $X = (x_1, x_2, \dots, x_n)$,
183 the M-K test statistic S is defined by:

184

$$S = \sum_{i=1}^{n-1} \sum_{j=i+1}^n \text{sgn}(x_j - x_i) \quad (3)$$

185 where n is the data record length, x_i and x_j are the sequential data values, and the function $\text{sgn}(x)$ is
186 defined as:

187

$$\text{sgn}(x) = \begin{cases} 1 & x > 0 \\ 0 & x = 0 \\ -1 & x < 0 \end{cases} \quad (4)$$

188 The statistic S is approximately normally distributed with the mean $E(S) = 0$ and variance as

189

$$\text{Var}(S) = \frac{n(n-1)(2n+5) - \sum_{i=1}^n t_i(i-1)(2i+5)}{18} \quad (5)$$

190 where t_i is considered as the number of ties up to sample i . The standardised normal test statistic Z is
191 given by

192

$$Z = \begin{cases} \frac{S-1}{\sqrt{\text{Var}(S)}} & S > 0 \\ 0 & S = 0 \\ \frac{S+1}{\sqrt{\text{Var}(S)}} & S < 0 \end{cases} \quad (6)$$

193 The null hypothesis H_0 that there is no trend in the records, is rejected (not rejected) if the
 194 statistic Z is greater (less) than the critical value of $Z_{\alpha/2}$ obtained at the level of significance α . A
 195 positive (negative) value of Z signifies an upward (downward) trend [Bao *et al.*, 2012].

196 Furthermore, the nonparametric Mann-Kendall's test can also be used to detect the change
 197 points of time series [Partal and Kahya, 2006]. This test sets up two series, a forward one (UF) and a
 198 backward one (UB). The UF is similar to the Z values that are calculated for the data. Following
 199 Partal and Kahya [2006], the steps are:

200 a) The magnitudes of x_i ($i = 1, 2, \dots, n$) mean time series are compared with x_j ($j = 1, 2, \dots, i-1$).

201 For each comparison, the number of cases $x_j > x_i$ is counted and denoted by r_i .

202 b) The test statistic S_k is

203

$$S_k = \sum_{i=1}^k r_i \quad (k=2,3,\dots,n) \quad (7)$$

204 c) The mean and variance of the test statistic are calculated as

205

$$E(S_i) = \frac{i(i-1)}{4} \quad (8)$$

206

$$\text{Var}(S_i) = \frac{i(i-1)(2i+5)}{72} \quad (9)$$

207 d) The sequential values of the statistic UF are computed as

208

$$UF_i = \frac{S_i - E(S_i)}{\sqrt{\text{Var}(S_i)}} \quad (i=1, 2, \dots, n) \quad (10)$$

209 Similarly, the values of UB are computed backward from the end of the time series. If the UF
 210 and UB curves intersect and then diverge and acquire specific threshold values, then a statistically

211 significant trend exists [Tabari *et al.*, 2011]. The point of intersection shows the approximate change
212 point at which the trend begins [Mosmann *et al.*, 2004].

213

214 2.2.3 Moving-average method

215 The simple moving-average method is typically used to test the trend in a long-time series [Zhai
216 *et al.*, 2014]. A moving-average method is used to smooth out short-term data fluctuations and
217 highlight longer-term trends. The moving-average method can be expressed as:

$$218 \quad F(t) = \frac{(x(t) + x(t-1) + \dots + x(t-(N-1)))}{N} \quad (11)$$

219 in which $x(t)$ is the actual value at time t of the original time series, N is the average periodicity, and
220 $F(t)$ indicates the predicted values of the t stage. The threshold between short-term and long-term
221 depends on the application, and the parameters of the simple moving-average method are set
222 accordingly. A commonly used five-year average is used in this study.

223

224 2.2.4 Spatial interpolation

225 Spatial interpolation as a necessary tool has been widely used in building precipitation
226 distribution from rain-gauge data. There are many methods available, such as Polynomial,
227 Nearest-neighbour, Inverse Distance Weighted (IDW), Kriging and its variants. The normal Kriging
228 method is selected for this study because it contains the highest correlation coefficient calculated
229 from the cross-validation test [Garen and Marks, 2005; Liang *et al.*, 2011a]. Moreover, this
230 technique also produced the closest representation of the real values, which was in the form of the
231 lowest difference between the observed and predicted values of known data points [Roy, 2009]. Thus,
232 Kriging is implemented on all 43 rain gauges to obtain the spatial pattern of precipitation in the study

233 area.

234

235 **3. Results**

236 3.1 Temporal variability and trends of precipitation amounts in the Beijing area

237 The mean annual precipitation from 1950-2012 varies from a low of 383.9 mm in 1965 to a
238 high of 1,005.6 mm in 1954, with a mean of 584.7 mm. A decrease in mean annual precipitation is
239 observed for Beijing after 1960. Although the mean annual precipitation exhibits large inter-annual
240 variability, it has decreased overall by almost 32% during this period at a rate of 28.5mm/10a (Figure
241 2). Five-year moving average curves emphasize the trends and variability in the annual precipitation
242 series. The decadal variability of precipitation indicates that alterations of wet and dry periods occur
243 over time. For example, 1954-1964 is a wet period followed by a gradual decrease of annual
244 precipitation to its long-term average value from 1965-1975. Another short wet period occurred from
245 1976-1979, exhibiting a narrow magnitude. Beijing experienced a relatively longer dry period in the
246 1980s and early 1990s, with 1980 being the third driest year during the 1950-2012 time period. A
247 transitory wet period in the mid-1990s occurred next, followed by another long and more severe dry
248 spell from 1997-2011, during which 1999 was the second driest year on record since 1950. As for the
249 maxima, Figure 2 also shows that the precipitation in 2012 exceeded 700 mm, the highest value in
250 the last 18 years and the second largest over the past three decades. The declining annual
251 precipitation trend in Beijing is consistent with the trends in the Haihe River basin [*Bao et al.*, 2012;
252 *Chu et al.*, 2010] as well as northern China in a larger context [*Cong et al.*, 2010] over the past 60
253 years. For seasonal precipitation, the warm-season (June-September) precipitation accounts for about
254 83.5% (60.13%-91.53%) of the annual precipitation from 1950-2012. The decreasing trend (29.7

255 mm/decade) of warm-season precipitation is consistent with that of annual precipitation (both
256 statistically significant at 0.05 significance level). At the seasonal level, precipitation in spring and
257 autumn shows a slowly increasing (statistically insignificant) trend of 0.7 mm/decade and 0.9
258 mm/decade, respectively, while the summer precipitation declined by 32.8 mm/decade (statistically
259 significant). In comparison, the trend of mean precipitation in winter shows little change, fluctuating
260 within a narrow range. Thus, we attribute to the fact that the steadily increasing trend in the spring
261 and autumn is unable to offset the remarkable decrease in the summer, which plays a dominant role
262 in the trends of overall annual precipitation.

263 A similar conclusion can also be drawn from Figure 3, which shows decadal changes in
264 precipitation according to seasons. Significant inter-decadal and inter-annual variations in
265 precipitation amounts are revealed. Mean and median values of summer, warm-season, and annual
266 precipitation from 2000-2012 are all lower than those of earlier decades. We also observe larger
267 inter-annual variations in the 1950s compared with other decades. In contrast, the mean and median
268 values in spring and autumn first decline from the 1950s and then rise in the 1980s. Additionally,
269 there is no stable variation pattern in winter, with a state of disorder.

270 [Figure 2 and Figure 3 should be inserted here]

271 The trends obtained by the M-K method are shown by the red (*UF*) and blue (*UB*) solid lines,
272 respectively, in Figure 4, and the horizontal dashed lines correspond to the confidence limits at the
273 significance level of $\alpha = 0.05$. A statistically significant trend of increasing or decreasing
274 precipitation is indicated if the red solid line crosses over the dashed line. There is no significant
275 trend for the autumn and winter (Figures 4c-4d), but a short-term significant decrease occurs for the
276 spring during the 1958-1963 and 1972-1979 periods (Figure 4a). Summer and warm-season

277 precipitation exhibit a declining trend for most years, particularly during the 1999-2012 period
278 (Figures 4b and 4e). The analogous trend occurs for annual precipitation, with the significant
279 decrease commencing in 2001 (Figure 4f).

280 Monthly precipitation amounts and their percentage shares of annual precipitation are displayed
281 in Figure 5. Results indicate that monthly precipitation patterns do not change significantly. It is clear
282 that a large proportion of annual precipitation amount occurs in the warm season (76.4-82.6%),
283 especially during July (27.5-36.8%) and August (21-31.8%). The maximum contributing months to
284 the annual precipitation amount vary for different decades. In the 1950s and 1980s, the August
285 contribution is larger than that from July, while in the other decades, the August contribution is less
286 than that from July. As discussed earlier, we also find that the contribution from both July and August
287 to the total precipitation shows a remarkable decreasing trend since the 1980s, while that of June and
288 September shows a slight increasing trend. Figure 5b clearly shows that the precipitation amount in
289 July (August) during 1980-2012 has a remarkable decreasing trend, ranging from 209.5 (191.3) mm
290 down to 167.3 (131.1) mm. Thus, the decreases in monthly contributions and precipitation amounts
291 for July and August are a dominant factor in the decreases in summer and warm-season precipitation.

292 [Figure 4 and Figure 5 should be inserted here]

293

294 3.2 Spatial characteristics of warm season precipitation

295 Precipitation records collected from 43 stations over the period of 1980-2009 are used to
296 analyze the inter-decadal spatial variations in warm season precipitation (Figure 6). The records are
297 further divided into three decades: 1980-1989, 1990-1999, and 2000-2009. In the 1980s (Figure 6a),
298 more precipitation occurs in the northeast mountainous area, with the highest totals of around 600

299 mm occurring at stations near HSY (591.5 mm) and ZLY (586.6 mm). A relatively high mean
300 precipitation amount (> 500 mm) is recorded for the plains areas of the northeastern part of the OSA.
301 In the SWMA and NWMA regions, the mean precipitation amount is usually less than 400 mm, with
302 the minimum precipitation less than 300 mm recorded at the GT station. We also find an increase in
303 precipitation in the central urban area around the SLZ and YAM stations, with the highest record
304 surpassing 450 mm.

305 For 1990-1999 (Figure 6b), the highest precipitation amount also occurs in the northeast near
306 the HSY station (≥ 600 mm); a secondary center of precipitation occurs at the Huairou and Miyun
307 reservoirs, with precipitation exceeding 550 mm. Similar to the 1980s, the precipitation amount in
308 the central urban area surpasses that of the suburb area, with the lowest values recorded for stations
309 located primarily in the NWMA and SWMA. However, it was found a small area with high amount
310 in the southwestern sub-region at the ZF station. Overall, there was more precipitation in the 1990s
311 than that of the 1980s, as shown in Figure 6d.

312 Since 2000 (Figure 6c), the mean maximum precipitation decreases to about 525 mm. On the
313 whole, spatial patterns of precipitation do not change appreciably between 1980 and 2009, indicating
314 only slight variations at the decadal level. Observed results show that precipitation amounts is higher
315 in the eastern part than in the west. Moreover, precipitation in the plains areas is greater than in the
316 mountainous areas, which is also concluded by *Zhai et al.* [2014]. Interestingly, the central urban
317 area does show a relatively greater precipitation amount, which may well be linked to the
318 urbanization effects and land use/cover change (an issue discussed later in Section 4.1).

319 Figure 6 also examines the decadal precipitation variation in terms of its spatial distribution
320 based on the 43 rain gauges. Overall, precipitation is declining after increasing during most of the

321 past three decades. This trend is similar to the changes in mean annual precipitation for the same
322 period discussed in Section 3.1, with the largest values occurring in the 1990s and the lowest in the
323 2000s. Compared to the 1980s, the total warm-season precipitation in the 1990s is greater, except for
324 a few areas in the northeast (Figure 6d). In the 2000s, the largest decreases occurred in the
325 northeastern areas, with the largest decrease (≥ 150 mm) occurring at the ZLY and PG stations
326 (Figures 6e-6f). Another major decrease in precipitation took place around the Miyun and Huairou
327 reservoirs, which decreased more than 100 mm since the 1990s (Figure 6e). Because the Miyun
328 reservoir supplies most of Beijing's water, this reduction in precipitation directly intensified the
329 metropolitan water shortage. Another significant decrease of more than 100 mm is observed in the
330 UA, which accounts for 20-30% of the mean warm-season total precipitation.

331 It is interesting to see the spatial distribution of the temporal trend at each rain-gauge station.
332 The M-K test results for warm-season precipitation amounts are presented in Figure 7. We found that
333 29 stations experienced a decreasing trend. Amongst these stations, which are located mainly in the
334 mountainous and outer suburb area, three stations (QJD, YQY, and PG) experienced by significantly
335 decreasing precipitation at the 95% confidence level. Fourteen stations exhibit increasing
336 precipitation (not statistically significant), and are mostly found mostly in the urban (6 stations
337 except for the YAM station) and inner suburb areas (7 stations). Figure 7 also reveals that most
338 stations located in the urban area are marked by non-significant increases in precipitation.

339 [Figure 6 and Figure 7 should be inserted here]

340 The changes in trends and variation of mean warm-season precipitation for the six sub-regions
341 from 1980-2012 are shown in Figure 8. In all six sub-regions, the precipitation amounts first increase
342 and then decline from 1980-2012. Except for the NWMA, the other five areas have one or two

343 change points. In general, the change points of the four plains areas occur at the end of the 1990s,
344 with the other change points in the ISAN occurring in 2011. The change point of the SWMA occurs
345 at the beginning of the 21st century, and those for the NWMA occur around the same time. The
346 precipitation amounts in the four plains areas exhibit a significant increasing trend towards the end of
347 the 1980s and/or the early 1990s at the level of $\alpha = 0.05$, especially for UA and ISAS (significant at
348 the level of $\alpha=0.01$). Moreover, the decreasing trends in the four plains areas in the 2000s are not
349 statistically significant at either of these two levels.

350 [Figure 8 should be inserted here]

351

352 3.3 Spatio-temporal characteristics of precipitation intensity

353 The precipitation intensity is another important quantity in our analysis as it is one of the key
354 factors in determining urban drainage design and flood control. In this study, two indices related to
355 precipitation intensity have been calculated and analyzed, namely the hourly precipitation intensity
356 and maximum 1hr precipitation intensity. Hourly precipitation intensity has been widely used by
357 climatologists to analyze variations in precipitation [Wang *et al.*, 2012b; Yang *et al.*, 2013];
358 maximum 1hr precipitation intensity is mostly used in flood control analysis and forecasting. The
359 definition of hourly precipitation intensity provided by Oke and Musiaka [1994] is used here. As the
360 term implies, the maximum 1hr precipitation is the maximum amount of precipitation that occurs
361 within a continuous one-hour in a year. To a certain extent, the maximum 1hr precipitation intensity
362 can be regarded as an index to examine the extreme precipitation events.

363 Overall, the spatial variations of precipitation intensity are similar to the spatial distribution of
364 precipitation amount (Figures 9a-9b). The higher values occur most frequently in the plains area,

365 whereas lower values are confined primarily to the mountainous areas. Figure 9a shows that the
366 greatest hourly mean precipitation intensity appears in the OSA near the MY and ZLY stations; the
367 next-highest values are located in the UA at the SLZ station and in the ISAS at the FS station. In
368 contrast, the lowest values occur in the NWMA near the YQ and QJD stations. As seen in Figure 9a,
369 we can conclude that the spatial pattern of hourly mean precipitation intensity is controlled mainly by
370 topographic factors. To some extent, the effect of urbanization may well be important as we have
371 seen relatively higher hourly mean precipitation intensity appearing in the built-up sections of the
372 metropolis. Similar findings are also obtained from Figure 9b, with the highest total found in the
373 outer suburb area near the MY station and the lowest total in the northwest mountainous area. The
374 reason may lie in the fact that the warm southeasterly and southwesterly winds are forced to rise
375 against the mountains of the west and the north, triggering heightened summer precipitation along
376 the windward slopes and reducing precipitation on the leeward slopes [Xu *et al.*, 2006b]. This can
377 also help to explain the precipitation concentrating in the windward slopes of the mountains
378 surrounding the plains area, such as the ZF, SJD, TYK, HR, MYB, and HSY stations, where the
379 maximum 1hr precipitation is more than 36 mm. Similar to the hourly mean precipitation intensity,
380 high values appear in the UA (SLZ, YAM, GBD and TX) and exceed 36 mm. Hence, the effect of
381 urbanization (e.g., urban heat island, land surface roughness, and aerosol density) on precipitation is
382 also important, and requires further investigation.

383 Figure 9 also shows the M-K statistical trends of hourly mean precipitation intensity and
384 maximum 1hr precipitation. For hourly mean precipitation intensity, only four among the 43 stations
385 exhibit a significantly increasing trend at the level of $\alpha = 0.05$. They are located mainly in the
386 transition zone between the mountainous and plains areas. We also find that the most stations in the

387 UA, NWMA and the southern part of the metropolis reveal a rising trend, although not statistically
388 significant, and that most of the stations are found to be downward-trending in the ISAN and OSA.
389 The increasing hourly mean precipitation intensity in the region implies that they are increasingly
390 concentrated in short-duration precipitation events, which concurs with previous studies [*Li et al.*,
391 2008; *Yang et al.*, 2013]. There are 25 stations with an upward trend in maximum 1hr precipitation
392 (Figure 9d), but two stations (WQ and XYL) display a significant upward trend at the level of $\alpha =$
393 0.05. The remaining 18 stations show a slight decreasing trend but without statistical significance.
394 We also find that most stations that record higher values in maximum 1hr precipitation, such as the
395 Miyun reservoir, the five stations in the central urban area, and the southern part of Beijing
396 metropolis, exhibit an upward trend.

397 [Figure 9 should be inserted here]

398 Another use of the M-K method is to assess trends in precipitation intensity for the six
399 sub-regions (Figures 10 and 11). Figure 10 shows the inter-annual and spatial variation of mean
400 hourly precipitation intensity. The results show a slowly increasing trend in four areas (UA, ISAS,
401 SWMA, and NWMA) and a decreasing trend in the other two areas (ISAN and OSA). Overall, apart
402 from SWMA, the inter-annual variation of the mean hourly precipitation intensity in the other five
403 areas first increases and then decreases. The lowest intensities occur at the end of the 1990s and the
404 beginning of the 2000s. However, the patterns for the UA, ISAS, ISAN, and NWMA shows another
405 increasing trend in the 2000s. Figure 10 also reveals that the mean hourly precipitation intensity in
406 the two mountainous areas has remained at a fairly stable level, while that of the plains areas exhibits
407 more fluctuation. Additionally, Figure 11 also shows the inter-annual variation of maximum 1hr
408 precipitation intensity during the warm season over the past three decades. On the whole, similar to

409 hourly mean precipitation intensity, the maximum 1hr precipitation first rises and then falls. There
410 are major declines in maximum 1hr precipitation in the UA, ISAS, and OSA during the longer-term
411 dry period beginning in 1999. The high amplitudes of this 1hr precipitation for all sub-regions and
412 for all time periods lead to significant changes regarding variance even though there are
413 non-statistically significant changes in mean values for the past three decades. This profile of change
414 is also observed in the inner suburb area (ISAS and ISAN) in the 2000s, together with a surge in
415 maximum 1hr precipitation intensity.

416 [Figure 10 and Figure 11 should be inserted here]

417

418 **4 Possible causes of changes in precipitation patterns**

419 It is well known that many factors shape precipitation variation in a region, especially in a large
420 urban area. Local precipitation variation is a response to global and regional water cycles, as well as
421 climate variation, the mechanism of which is highly complicated and beyond the scope of this
422 research. In addition, local factors — such as terrain, urbanization, land use/cover change — produce
423 their own spatial impacts on the precipitation pattern. In this section, we discuss possible causes by
424 first making comparisons to regional precipitation change and then qualitatively analyzing the
425 impacts of topography and urban expansion on precipitation.

426

427 4.1 Regional and local climate conditions

428 Over the past 50 years, precipitation has increased in the northwestern and southern China, but
429 has decreased in northern China [*Cong et al.*, 2010; *Liu et al.*, 2005; *Zhai et al.*, 2005]. Annual
430 precipitation has decreased by about 5% per decade in northern China because onshore monsoon

431 winds have become weaker and water vapor transfer has diminished [*Cong et al.*, 2010; *Xu et al.*,
432 2006a]. High rise buildings associated with urbanization and temperature differences may also cause
433 wind speed reduction [*Cong et al.*, 2010; *Ren et al.*, 2008]. The decline of precipitation in Beijing is
434 consistent with observations all across in northern China, especially in the Haihe River basin where
435 the city is located. Seasonal precipitation change discussed earlier also comes into play: the
436 significant decrease in summer precipitation and warm-season precipitation, in particular, is a leading
437 contributor to the annual precipitation decline in Beijing (Figures 2 and 3). Although the spring and
438 autumn precipitation exhibit a slightly increasing trend, it cannot offset the decline in summer
439 precipitation and annual precipitation. This is consistent with the work of *Zhai et al.* [2005], which
440 addresses observations for spring and summer, but contradicts their findings for autumn and winter
441 in northern China. According to *Hao et al.* [2007, 2011], the causes of declining summer
442 precipitation in northern China are: (1) the weakening of the Mongolian low, and (2) the decline of
443 water vapor transportation from the southwest wind flow because of the depleting movement of
444 southwest monsoon and southeasterly winds from the western Pacific subtropical high. To some
445 extent, these factors may be the cause of the precipitation decline in the Beijing metropolis. *Wang et*
446 *al.* [2008] analyzed the temporal and spatial characteristics of precipitation and their statistical
447 relationship to SHWP (Subtropical High over the West Pacific). They found that the impact of the
448 SHWP on precipitation in Beijing displayed a significant interdecadal trend, with most rainstorms
449 steered by the combination of the SHWP and westerly trough. Although the causes of precipitation
450 variation in Beijing are still not fully understood, changes in regional atmospheric circulation
451 obviously play a role and require further investigation. In addition, a worldwide review of global
452 rainfall data has found that the intensity of most extreme precipitation events is increasing across the

453 globe as temperatures rise [*Alexander et al.*, 2006; *Westra et al.*, 2013]. Another avenue of research
454 involves temperature from work by *Zhu et al.* [2012], which knows that the mean temperature in
455 Beijing has increased significantly since the 1950s (Figure 12a).

456 [Figure 12 should be inserted here]

457

458 4.2 Topography impacts

459 *Smith* [1979] has comprehensively reviewed the complex subject of orographic rainfall. On the
460 windward side, forced lifting of air masses triggers condensation and precipitation with increasing
461 elevation. Depending on the mountain size and the efficiency of the release processes, precipitation
462 will decrease on the leeward side. Thus, topography strongly influences precipitation patterns by
463 altering both the local wind patterns and the condensation of perceptible water [*Siler and Roe*, 2014;
464 *Smith*, 1979]. Beijing has a typical continental monsoon climate with four distinct seasons. The
465 winter is cold and dry due to northerly winds from high-latitude areas, while the summer is hot and
466 wet because of the east and southeast airflow carrying moisture from the southern Pacific Ocean and
467 the Indian Ocean. Because mountainous areas are located primarily in the northern and western
468 sections of Beijing, precipitation in the low-lying southern and eastern parts of Beijing is greater than
469 that of the western and northern sections. We discovered that the highest precipitation occurs at the
470 interface between the mountainous area and the plains areas, confirming the effect of terrain on
471 precipitation patterns. Data from our rain gauges verify these results, which are corroborated further
472 in the findings we observed for changes in precipitation intensity. However, the specific interactions
473 occurring between the topography and the local climate, which contribute to the unique spatial
474 distribution of precipitation among the various regions, has not been fully understood or examined

475 due to lack of adequate data.

476

477 4.3 Urbanization impacts

478 Urban expansion is known to affect precipitation and previous studies have noted that the
479 amount and frequency of precipitation tends to be greater in urban centers and downwind areas than
480 in the surrounding areas, especially for intense convective precipitation in the summer [*Ganeshan et*
481 *al.*, 2013; *Zheng and Liu*, 2008]. However, this phenomenon has not been confirmed for Beijing in
482 research by *Wang et al.* [2009] and *Liang et al.* [2011b]. *Xu et al.* [2009] and *Li and Ma* [2011] did
483 observe that the urban effect was apparent for large-scale weak precipitation and local strong
484 precipitation, but it could not be discerned for large-scale intense precipitation events. *Yin et al.*
485 [2011] concluded that Beijing precipitation patterns might be shaped by the combined influences of
486 mountain-valley topography and urbanization. *Wang et al.* [2012a] found that the magnitude of
487 precipitation increases slightly in the Beijing-Tianjin urban areas, and argued that urbanization has
488 the greatest impact on summertime precipitation. In our study, we found that the precipitation within
489 the metropolis is greater than the total in surrounding areas during the 1980s and 1990s, whereas
490 warm-season precipitation in the central urban area decreased by about 100 mm from the 1990s to
491 2000s and by 60-80 mm from the 1980s to the 2000s (see Figure 7). As shown in Figure 12b, urban
492 development in Beijing increased at an annual increment of 8.453 km² from 1980-2000, while the
493 increased in rate is more substantial after 2000, approximate at 48.751 km², indicating a rapid urban
494 expansion of Beijing in the 2000s, especially before the 2008 Beijing Olympics. There is a slightly
495 increasing trend of in mean warm-season precipitation over the whole Beijing area from 1980-2000,
496 fluctuating with an increment of 1.033 mm per year. Such a trend is more pronounced from

497 2000-2012, fluctuating with a linear variation of 12.213 mm per year, whereas such an increasing
498 trend of warm-season precipitation for the UA is more evident (increasing at a rate of 2.077 mm per
499 year from 1980-2000, and 20.633 mm per year from 2000-2012).

500 Short-duration heavy precipitation events have been occurring more frequently in Beijing
501 during the past few years [You *et al.*, 2014; Zhang and You, 2013]. For instance, the heaviest
502 precipitation in 60 years occurred on July 21, 2012, with a record-breaking amount of 460 mm in 18
503 hours and maximum hourly rainfall rates in excess of 85 mm [Huang *et al.*, 2014; Wang *et al.*, 2013;
504 Zhang *et al.*, 2013a]. Zheng *et al.* [2013] found that the frequency of extreme precipitation events
505 gradually decreased from west to east from 1971-2010, and that the impact of urbanization on
506 precipitation intensity and frequency of extreme precipitation events had become even more apparent.
507 A similar assessment was also provided by Li and Ma [2011]. Yang *et al.* [2014] investigated the
508 climatology of summer heavy rainfall events over the Beijing area, confirming that there are two hot
509 spots of higher frequency of summer heavy rainfall events, including the urban core region and the
510 climatological downwind region. However, our findings showed that, although there was an obvious
511 decline in precipitation amount, mean hourly precipitation intensity did not exhibit a significant trend
512 from 1980-2012. Nonetheless, there is an increasing trend at a rate of 0.1 mm/h per year during the
513 2000-2012 period (which saw especially rapid urban expansion) in the UA (see Figure 10). That
514 trend was more pronounced in the ISAS, fluctuating with a linear variation of 0.16 mm/h per year.
515 We also found that the maximum 1hr precipitation increased from 1980-2012, especially in the
516 transition zone, where the mountains meet the plains area and the UA (see Figures 9 and 11).

517 It should also be noted that urban heat island effects also constitute an important factor. In
518 urbanized areas, sizeable quantities of anthropogenic heat are generated by human activities [Zhang

519 *et al.*, 2013b]. Moreover, growing energy consumption exacerbates local environmental problems, as
520 well as reinforcing temperature increases in the urban atmosphere. Furthermore, the radiative
521 properties of the urban environment are distinctly different, allowing the absorption of additional
522 radiation due to the nature of the urban canopy [*Aikawa et al.*, 2009]. Such changes in the surface
523 heat budget produce atmospheric conditions in urbanized areas that are quite different from those in
524 rural areas, and significantly impact local air circulation and patterns of precipitation [*Huong and*
525 *Pathirana*, 2013]. *Zhang et al.* [2009] found that urban expansion produces less evaporation, higher
526 surface temperatures, larger sensible heat fluxes, and a deeper boundary layer, which leads to less
527 water vapor, more mixing of water vapor in the boundary layer, and reduces precipitation in Beijing.
528 In our analysis, the effect of urbanization on precipitation intensity has manifested itself in a slightly
529 increasing trend in the mean hourly precipitation intensity and maximum 1hr precipitation intensity
530 in the urban areas. Several other causal factors are known to exist such as large surface roughness
531 and higher aerosol concentration, but their impacts could not be examined in this study because of
532 the lack of data for the Beijing metropolitan area.

533

534 **5 Implication for water crises**

535 Beijing is already well known as one of the world's most water-challenged cities because of its
536 enormous urban population (more than 20 million) and relatively low average precipitation
537 (averaging about 585 mm during 1950-2012). In comparison, Shanghai, a city with a population 25%
538 larger than Beijing, has an annual precipitation of 1,150 mm (1950-2010 average). Given our finding
539 that precipitation has significantly decreased in Beijing since the 1950s, this trend increasingly
540 exacerbates the city's water shortage, in particular, capita water availability has declined from about

541 1,000 m³ in 1949 to 100 m³ in 2009. Certainly, drought further intensifies this water crisis - Beijing
542 has endured 30 years of below-average precipitation since the 1980s and 13 consecutive dry years
543 from 1999-2011). For example, the Guanting Reservoir currently receives only a fraction of the
544 water it received in the 1950s, and the inflow of the Miyun Reservoir has been steadily declining
545 over the past 20 years (see Figure 13). More specifically, the Guanting Reservoir received 99% less
546 water in 2012 compared to the 1950s, with rivers now dry for most of the year downstream of the
547 reservoir. To cover the supply deficit, unprecedented amounts of ground water are pumped to the
548 surface and now accounts for more than two-thirds of the entire water supply. It is not surprising that
549 this massive ground-water extraction is occurring at a pace faster than it can be recharged, resulting
550 in a sharp drop in the ground-water table (see Figure 13). A report by the *Probe International Beijing*
551 *Group* [2008] stated that an estimated six billion cubic meters of groundwater above the safe limit
552 have been extracted and may never be replenished. A particular concern is that on a rising number of
553 occasions water supplied from rivers (e.g., the Yongding River) and reservoirs (e.g., the Guanting
554 reservoir) needed to be temporarily abandoned as a source of drinking water because of deteriorating
555 water quality and pollution [Bao and Fang, 2012], resulting in the exacerbation of intense water
556 scarcity in the Beijing area.

557 The Chinese government's main response to Beijing's water crisis is to expand the supply by
558 tapping ever-deeper groundwater, diverting surface-water resources via the massive South-North
559 Water Diversion, accelerating and sea-water desalination, increasing the use of reclaimed water,
560 shutting down or relocating polluting and water-intensive factories, and restricting the water use in
561 neighboring provinces. Since open-ended supply expansion is not a permanent solution of the water
562 crisis, other measures also need to be pursued. For example, water conservation in industry and

563 agriculture can compensate for these losses and free up more water for residential uses. Water
564 charges can be increased to provide an incentive to curb residential water use (efforts to date have
565 been quite limited). Institutional reforms to promote integrated management of water systems have
566 been undertaken recently and need to be expanded. They include restructuring water consumption
567 and water-use patterns (see Figure 14).

568 [Figure 13 and Figure 14 should be inserted here]

569 Changes in global and local climate can affect regional water resources by altering the amount
570 and distribution of precipitation in a given area [*Labat et al.*, 2004]. In this regard, urban areas are
571 emerging as “first responders” to accommodate and mitigate climate change [*Mishra et al.*, 2012;
572 *Rosenzweig et al.*, 2010]. Changes in extreme precipitation may pose challenges for urban
573 storm-water management, because existing facilities were designed under the assumption of climate
574 stationarity [*Milly et al.*, 2008]. Another consequence of the increase in extreme precipitation events
575 is widening damage caused by floods [*Roy*, 2009]. Statistics published by the Beijing Hydrological
576 Stations of the Beijing Water Authority show that 37 local heavy precipitation events (those with
577 maximum 1hr precipitation intensities greater than 70mm) occurred in metropolitan Beijing during
578 the period of 2004-2012. These events heighten the possibility of urban flooding, which is
579 aggravated by an outdated urban drainage system than cannot handle the discharges, therefore
580 requiring the modernization and redesign of these facilities [*Zawilski and Brzezińska*, 2013]. A
581 tendency of more intense precipitation has been predicted, and serious problems for urban drainage
582 are expected in the near future. The contradiction or non-conformity between the frequency of
583 precipitation intensity in a changing environment and design standards of urban drainage systems
584 may be an important reason for the increasing world-wide urban flood and inundation in recent years,

585 especially for those cities in developing countries. Beijing's drainage system also has some
586 fundamental flaws because its original designs prioritized the importance of roads and buildings,
587 rather than actual drainage needs. Generally, the design of urban drainage systems is mostly based on
588 precipitation and corresponding storm-water discharge, with certain return periods ranging from 5 to
589 100 years [Mishra *et al.*, 2012]. However, such design in Beijing is based on precipitation with return
590 periods of around three years (sources: Beijing Water Authority), which is lower than that of many
591 large metropolitan areas, including New York, Tokyo, Paris, and London. This low design standard
592 may be another major cause of heightened urban flooding in recent years. Hence, the Beijing
593 municipal government proposed many additional structural measures to modify the drainage system
594 to handle flood events of return intervals between 3-10 years. Moreover, because urban drainage
595 catchments are relatively small and marked by substantial impervious or semi-pervious surfaces,
596 their response times to extreme precipitation are usually short. Therefore, the intensity and durations
597 of precipitation are both key factors for urban drainage network design [Li *et al.*, 2008; Wang *et al.*,
598 2012b; Yin *et al.*, 2011]. Both factors can be significantly affected by further urbanization and
599 expansion of the impervious areas in the future.

600

601 **6. Conclusions**

602 This study has investigated trends in the spatio-temporal variation of precipitation patterns in
603 the Beijing metropolitan area using both the long-time series of annual precipitation during the
604 period 1950-2012 and the relatively short-time series of daily precipitation at 43 rain gauges from
605 1980-2012. Based on our analysis, we draw the following conclusions:

606 1) Within the Beijing metropolis, annual precipitation has significantly decreased from 1950-2012

607 (by almost 32%). Seasonally, a higher decrease in precipitation occurred in the summer and
608 warm season, with a slight increase in spring and autumn precipitation. However, this increase is
609 unable to offset the remarkable decrease in summer and warm-season precipitation, which is the
610 main source of the decline in mean annual precipitation.

611 2) In general, precipitation in the plains areas is greater than that in the mountainous areas of the
612 metropolis, with the highest values occurring in the northeastern part near the Miyun and Huairou
613 reservoirs. A secondary peak is noted in the eastern part of the outer suburb area.

614 3) Except for a single sub-region (SWMA), slightly increasing trends to decreasing trends in hourly
615 mean precipitation intensity and maximum 1hr precipitation intensity were observed during the
616 warm season in Beijing, and the changing point occurred at the end of the 1990s and the
617 beginning of the 2000s. Similar to the warm-season precipitation during the same period, there
618 are two hot spots of greater incidence of mean hourly precipitation intensity and maximum 1hr
619 precipitation. One hot spot is located in the central urban area, and the other is located in the
620 topographic transition zone in the northeast.

621 4) Changes in Beijing's precipitation are influenced by many factors, which include local climate
622 conditions, topographical effect, and the expanding urban landscape. The amount and intensity of
623 precipitation in the plains areas is greater than in the mountainous areas, and precipitation in the
624 urban areas is relatively greater than in the suburb areas.

625 5) Decreasing precipitation amounts in Beijing, especially around the Miyun Reservoir in the
626 northeast, will worsen the already troubled local water supply. In the mean time, higher
627 precipitation intensity elevates the risk of urban flooding [Wang *et al.*, 2013; You *et al.*, 2014]. All
628 of these factors pose new and severe challenges for water-resources management under the

629 growing impact of climate change and human activities.

630

631 **Acknowledgements**

632 Rainfall data to support this article are available from the Hydrological Data of Haihe River Basin (in
633 Chinese), the Annual Hydrological Report of China (Volume: III), released by Ministry of Water
634 Resources of China. For further information or right to access to the material used in this paper,
635 readers can also contact the Beijing Hydrological Center (<http://www.bjswzz.com/>) of the Beijing
636 Water Authority (<http://www.bjwater.gov.cn/pub/bjwater/index.html>). Weather data supporting
637 Figure 12a are available as in Supporting Information Table S1. For annual precipitation, urban
638 development and water resources data used in this article, readers can contact the corresponding
639 author X. Song. This study was supported by the National Basic Research Program of China
640 (2010CB951103), the Postgraduate Dissertation Foundation of the Nanjing Hydraulic Research
641 Institute (LB51302), and the National Natural Science Foundation of China (L1322014, 41330854,
642 41371063, and 51309155). We are thankful to the Beijing Hydrological Stations, Beijing Water
643 Authority for providing the precipitation data. We are also grateful to Prof. Xuesong Zhang, Pacific
644 Northwest National Laboratory and University of Maryland for his suggestions. We also thank the
645 editor Prof. L. Ruby Leung and three anonymous reviewers for their constructive suggestions and
646 comments, which were most helpful in improving this article. We are also very grateful to Dr. Peter
647 Muller for all the editorial suggestions he made for significantly improving the paper.

648

649 **References**

650 Aikawa, M., T. Hiraki, and J. Eiho (2009), Change of atmospheric condition in an urbanized area of Japan from the
651 viewpoint of rainfall intensity, *Environ Monit Assess*, 148(1-4), 449-453, doi:10.1007/s10661-008-0174-0.

652 Alexander, L. V., et al. (2006), Global observed changes in daily climate extremes of temperature and precipitation,

653 *Journal of Geophysical Research*, 111(D5), doi:10.1029/2005jd006290.

654 Allamano, P., P. Claps, F. Laio, and C. Thea (2009), A data-based assessment of the dependence of short-duration
655 precipitation on elevation, *Physics and Chemistry of the Earth*, 34(10-12), 635-641, doi:10.1016/j.pce.2009.01.001.

656 Bao, C., and C.-I. Fang (2012), Water Resources Flows Related to Urbanization in China: Challenges and Perspectives
657 for Water Management and Urban Development, *Water Resources Management*, 26(2), 531-552,
658 doi:10.1007/s11269-011-9930-y.

659 Bao, Z., J. Zhang, G. Wang, G. Fu, R. He, X. Yan, J. Jin, Y. Liu, and A. Zhang (2012), Attribution for decreasing
660 streamflow of the Haihe River basin, northern China: Climate variability or human activities?, *Journal of Hydrology*,
661 460-461, 117-129, doi:10.1016/j.jhydrol.2012.06.054.

662 Berne, A., G. Delrieu, J. Creutin, and C. Obled (2004), Temporal and spatial resolution of rainfall measurements required
663 for urban hydrology, *Journal of Hydrology*, 299(3-4), 166-179,
664 doi:10.1016/S0022-1694(04)00363-4|10.1016/j.jhydrol.2004.08.002.

665 Chu, H. (2012), Assessing the relationships between elevation and extreme precipitation with various durations in
666 southern Taiwan using spatial regression models, *Hydrological Processes*, 26(21), 3174-3181, doi:10.1002/hyp.8403.

667 Chu, J., J. Xia, C. Xu, L. Li, and Z. Wang (2010), Spatial and temporal variability of daily precipitation in Haihe River
668 basin, 1958–2007, *Journal of Geographical Sciences*, 20(2), 248-260, doi:10.1007/s11442-010-0248-0.

669 Chu, M. L., J. H. Knouft, A. Ghulam, J. A. Guzman, and Z. Pan (2013), Impacts of urbanization on river flow frequency:
670 A controlled experimental modeling-based evaluation approach, *Journal of Hydrology*, 495, 1-12,
671 doi:10.1016/j.jhydrol.2013.04.051.

672 Cong, Z., J. Zhao, D. Yang, and G. Ni (2010), Understanding the hydrological trends of river basins in China, *Journal of*
673 *Hydrology*, 388(3-4), 350-356, doi:10.1016/j.jhydrol.2010.05.013.

674 Creamean, J. M., et al. (2013), Dust and biological aerosols from the Sahara and Asia influence precipitation in the
675 western U.S., *Science*, 339(6127), 1572-1578, doi:10.1126/science.1227279.

676 Dai, A. (2013), Increasing drought under global warming in observations and models, *Nature Climate Change*, 3(1),
677 52-58, doi:10.1038/nclimate1633.

678 Damberg, L., and A. AghaKouchak (2014), Global Trends and Patterns of Droughts from Space, *Theor. Appl. Climatol.*,
679 doi:10.1007/s00704-013-1019-5.

680 Du, J. K., L. Qian, H. Y. Rui, T. H. Zuo, D. P. Zheng, Y. P. Xu, and C. Y. Xu (2012), Assessing the effects of urbanization
681 on annual runoff and flood events using an integrated hydrological modeling system for Qinhuai River basin, China,
682 *Journal of Hydrology*, 464, 127-139, doi:10.1016/j.jhydrol.2012.06.057.

683 Fletcher, T. D., H. Andrieu, and P. Hamel (2013), Understanding, management and modelling of urban hydrology and its
684 consequences for receiving waters: A state of the art, *Advances in Water Resources*, 51, 261-279,
685 doi:10.1016/j.advwatres.2012.09.001.

686 Ganeshan, M., R. Murtugudde, and M. L. Imhoff (2013), A multi-city analysis of the UHI-influence on warm season

687 rainfall, *Urban Climate*, 6, 1-23, doi:10.1016/j.uclim.2013.09.004.

688 Garen, D., and D. Marks (2005), Spatially distributed energy balance snowmelt modelling in a mountainous river basin:
689 estimation of meteorological inputs and verification of model results, *Journal of Hydrology*, 315(1-4), 126-153,
690 doi:10.1016/j.jhydrol.2005.03.026.

691 Grimm, N. B., S. H. Faeth, N. E. Golubiewski, C. L. Redman, J. Wu, X. Bai, and J. M. Briggs (2008), Global change and
692 the ecology of cities, *Science*, 319(5864), 756-760, doi:10.1126/science.1150195.

693 Han, J.-Y., J.-J. Baik, and H. Lee (2014a), Urban impacts on precipitation, *Asia-Pacific Journal of Atmospheric Sciences*,
694 50(1), 17-30, doi:10.1007/s13143-014-0016-7.

695 Han, J. Y., and J. J. Baik (2008), A theoretical and numerical study of urban heat island-induced circulation and
696 convection, *Journal of the Atmospheric Sciences*, 65(6), 1859-1877, doi:10.1175/2007JAS2326.1.

697 Han, Z., Z. Yan, Z. Li, W. Liu, and Y. Wang (2014b), Impact of urbanization on low-temperature precipitation in Beijing
698 during 1960–2008, *Advances in Atmospheric Sciences*, 31(1), 48-56, doi:10.1007/s00376-013-2211-3.

699 Hao, Z., A. AghaKouchak, and T. J. Phillips (2013), Changes in concurrent monthly precipitation and temperature
700 extremes, *Environmental Research Letters*, 8(3), 034014, doi:10.1088/1748-9326/8/3/034014.

701 Hao, L., J. Min, and X. Yao (2007), Analysis on the causes resulting in the reduction of summer rainfall over North China,
702 *Arid Zone Research*, 24(4), 522-527. (in Chinese)

703 Hao, L., J. Min, and Y. Ding (2011). Analysis of precipitation events changes and causes for rainstorm events reduction in
704 North China. *Chinese J. Geophys.*, 54(5), 1160-1167. doi: 10.3969/j.issn.0001-5733.2011.05.003

705 Huang, Y., et al. (2014), Evaluation of Version-7 TRMM Multi-Satellite Precipitation Analysis Product during the Beijing
706 Extreme Heavy Rainfall Event of 21 July 2012, *Water*, 6(1), 32-44, doi:10.3390/w6010032.

707 Huong, H. T. L., and A. Pathirana (2013), Urbanization and climate change impacts on future urban flooding in Can Tho
708 city, Vietnam, *Hydrology and Earth System Sciences*, 17(1), 379-394, doi:10.5194/hess-17-379-2013.

709 Jackson, C. R. (2011), Identification and quantification of the hydrological impacts of imperviousness in urban
710 catchments: A review, *Journal of Environmental Management*, 92(6), 1438-1448, doi:10.1016/j.jenvman.2011.01.018.

711 Kaufmann, R. K., K. C. Seto, A. Schneider, Z. Liu, L. Zhou, and W. Wang (2007), Climate Response to Rapid Urban
712 Growth: Evidence of a Human-Induced Precipitation Deficit, *Journal of Climate*, 20(10), 2299-2306,
713 doi:10.1175/jcli4109.1.

714 Kendall, M. G. (1975), Rank correlation methods, Griffin, Londn, UK

715 Labat, D., Y. Godd eris, J. L. Probst, and J. L. Guyot (2004), Evidence for global runoff increase related to climate
716 warming, *Advances in Water Resources*, 27(6), 631-642, doi:10.1016/j.advwatres.2004.02.020.

717 Ladson, A. R., C. J. Walsh, and T. D. Fletcher (2006), Improving stream health in urban areas by reducing runoff
718 frequency from impervious surfaces, *Australian Journal of Water Resources*, 10(1), 23-33.

- 719 Li, J., R. Yu, and J. Wang (2008), Diurnal variations of summer precipitation in Beijing, *Chinese Science Bulletin*, 53(12),
720 1933-1936, doi:10.1007/s11434-008-0195-7.
- 721 Li, S. Y., and J. J. Ma (2011), Impact of urbanization on precipitation in Beijing area, *Journal of the Meteorological*
722 *Sciences*, 31(4), 414-421.
- 723 Li, W., S. Chen, G. Chen, W. Sha, C. Luo, Y. Feng, Z. Wen, and B. Wang (2011), Urbanization signatures in strong versus
724 weak precipitation over the Pearl River Delta metropolitan regions of China, *Environmental Research Letters*, 6(3),
725 034020, doi:10.1088/1748-9326/6/3/034020.
- 726 Li, X., W. Zhou, and Z. Ouyang (2013), Forty years of urban expansion in Beijing: What is the relative importance
727 of physical, socioeconomic, and neighborhood factors?, *Applied Geography*, 38, 1-10, doi:10.1016/j.apgeog.2012.11.004.
- 728 Liang, L., L. Li, and Q. Liu (2011a), Precipitation variability in Northeast China from 1961 to 2008, *Journal of*
729 *Hydrology*, 404(1-2), 67-76, doi:10.1016/j.jhydrol.2011.04.020.
- 730 Liang, L. J., Z. S. Yang, and G. Y. Bai (2011b), Discussion on influence of urbanization on precipitation in Beijing,
731 *Beijing Water*(3), 15-18.
- 732 Liu, B., M. Xu, M. Henderson, and Y. Qi (2005), Observed trends of precipitation amount, frequency, and intensity in
733 China, 1960–2000, *Journal of Geophysical Research*, 110(D8), doi:10.1029/2004JD004864.
- 734 Lloyd, C. (2005), Assessing the effect of integrating elevation data into the estimation of monthly precipitation in Great
735 Britain, *Journal of Hydrology*, 308(1-4), 128-150, doi:10.1016/j.jhydrol.2004.10.026.
- 736 Luce, C., J. Abatzoglou, and Z. Holden (2013), The Missing Mountain Water: Slower Westerlies Decrease Orographic
737 Enhancement in the Pacific Northwest USA, *Science*, 342(6164), 1360-1364, doi:10.1126/science.1242335.
- 738 Mann, H. B. (1945), Nonparametric tests against trend, *Econometrica*, 13, 245-259
- 739 Miao, S. G., F. Chen, M. A. Lemone, M. Tewari, Q. C. Li, and Y. C. Wang (2009), An Observational and Modeling Study
740 of Characteristics of Urban Heat Island and Boundary Layer Structures in Beijing, *J. Appl. Meteorol. Climatol.*, 48(3),
741 484-501, doi:10.1175/2008jamc1909.1.
- 742 Miao, S. G., F. Chen, Q. C. Li, and S. Y. Fan (2011), Impacts of urban processes and urbanization on summer
743 precipitation: A case study of heavy rainfall in Beijing on 1 August 2006, *J. Appl. Meteorol. Climatol.*, 50(4): 806-825,
744 doi: 10.1175/2010JAMC2513.1
- 745 Miller, M. D. (2012), The impacts of Atlanta's urban sprawl on forest cover and fragmentation, *Appl. Geogr.*, 34, 171-179,
746 doi:10.1016/j.apgeog.2011.11.010.
- 747 Milly, P. C., J. Betancourt, M. Falkenmark, R. M. Hirsch, Z. W. Kundzewicz, D. P. Lettenmaier, and R. J. Stouffer (2008),
748 Stationarity is dead: whither water management?, *Science*, 319(5863), 573-574, doi:10.1126/science.1151915.
- 749 Mishra, V., F. Dominguez, and D. P. Lettenmaier (2012), Urban precipitation extremes: How reliable are regional climate
750 models?, *Geophys. Res. Lett.*, 39(3), doi:10.1029/2011gl050658.
- 751 Mosmann, V., A. Castro, R. Fraile, J. Dessens, and J. L. Sánchez (2004), Detection of statistically significant trends in the

752 summer precipitation of mainland Spain, *Atmos. Res.*, 70(1), 43-53, doi:10.1016/j.atmosres.2003.11.002.

753 Oke, T. R. (1973), City size and the urban heat island, *Atmos. Environ.*, 7(8), 769-779,
754 doi:10.1016/0004-6981(73)90140-6.

755 Oke, T.R., and K. Muusiake (1994), Seasonal change of the diurnal cycle of precipitation over Japan and Malaysia, *J.*
756 *Appl. Meteor.*, 33, 1445-1463.

757 Partal, T., and E. Kahya (2006), Trend analysis in Turkish precipitation data, *Hydrol. Process.*, 20, 2011-2026

758 Pathirana, A., H. B. Deneke, W. Veerbeek, C. Zevenbergen, and A. T. Banda (2014), Impact of urban growth-driven
759 landuse change on microclimate and extreme precipitation — A sensitivity study, *Atmos. Res.*, 138, 59-72,
760 doi:10.1016/j.atmosres.2013.10.005.

761 Pinto, O., I. R. C. A. Pinto, and M. A. S. Ferro (2013), A study of the long-term variability of thunderstorm days in
762 southeast Brazil, *Journal of Geophysical Research: Atmospheres*, 118(11), 5231-5246, doi:10.1002/jgrd.50282.

763 Probe International Beijing Group (2008), Beijing's water crisis 1949-2008 Olympics, June 2008.
764 <http://journal.probeinternational.org/2008/06/26/beijings-water-crisis-1949-2008-olympics/>

765 Ren, G., Y. Zhou, Z. Chu, J. Zhou, A. Zhang, J. Guo, and X. Liu (2008), Urbanization Effects on Observed Surface Air
766 Temperature Trends in North China, *Journal of Climate*, 21(6), 1333-1348, doi:10.1175/2007jcli1348.1.

767 Rosenzweig, C., W. Solecki, S. A. Hammer, and S. Mehrotra (2010), Cities lead the way in climate-change action, *Nature*,
768 467(7318), 909-911, doi:10.1038/467909a.

769 Roy, S. S. (2009), A spatial analysis of extreme hourly precipitation patterns in India, *Int. J. Climatol.*, 29(3), 345-355,
770 doi:10.1002/joc.1763.

771 Russell, A., and M. Hughes (2012), Is the changing precipitation regime of Manchester, United Kingdom, driven by the
772 development of urban areas?, *International Journal of Climatology*, 32(6), 967-974, doi:10.1002/joc.2321.

773 Seto, K. C., M. Fragkias, B. Guneralp, and M. K. Reilly (2011), A meta-analysis of global urban land expansion, *PLoS*
774 *One*, 6(8), e23777, doi:10.1371/journal.pone.0023777.

775 Siler, N., and G. Roe (2014), How will orographic precipitation respond to surface warming? An idealized thermodynamic
776 perspective, *Geophys. Res. Lett.* 41, 2606-2613. doi:10.1002/2013GL059095.

777 Smith, R. B. (1979), The influence of mountains on the atmosphere, *Adv. Geophys.*, 21, 87-230. DOI:
778 10.1016/S0065-2687(08)60262-9

779 Sun, J. S., and B. Yang (2008), Meso- β scale torrential rain affected by topography and the urban circulation, *Chinese*
780 *Journal of Atmospheric Sciences*, 32(6), 1352-1364.

781 Tabari, T., B. S. Somee, and M. R. Zadeh (2011), Testing for long-term trends in climatic variables in Iran, *Atmos. Res.*,
782 100(1), 132-140. DOI: 10.1016/j.atmosres.2011.01.005

783 United Nations, D. o. E. a. S. A. (2012), World Urbanization Prospects – the 2011 Revision *Rep.*, New York.

784 Wang, J., J. Feng, Z. Yan, Y. Hu, and G. Jia (2012a), Nested high-resolution modeling of the impact of urbanization on
785 regional climate in three vast urban agglomerations in China, *Journal of Geophysical Research: Atmospheres*, 117(D21),
786 n/a-n/a, doi:10.1029/2012JD018226.

787 Wang, J., R. Zhang, and Y. Wang (2012b), Areal differences in diurnal variations in summer precipitation over Beijing
788 metropolitan region, *Theor. Appl. Climatol.*, 110(3), 395-408, doi:10.1007/s00704-012-0636-8.

789 Wang, K., L. Wang, Y.-M. Wei, and M. Ye (2013), Beijing storm of July 21, 2012: observations and reflections, *Natural*
790 *Hazards*, 67(2), 969-974, doi:10.1007/s11069-013-0601-6.

791 Wang, X. Q., Z. F. Wang, Y. B. Qi, and H. Guo (2009), Effect of urbanization on the winter precipitation distribution in
792 Beijing area, *Sci. China Ser. D-Earth Sci.*, 52(2), 250-256, doi:10.1007/s11430-009-0019-x.

793 Wang, X., W. Wang, H. Liu, and H. Wang (2008), Beijing region precipitation feature and some statistics of relationship
794 between it and SHWP, *Plateau Meteorology*, 27(4), 822-829. (in Chinese)

795 Westra, S., L. V. Alexander, and F. W. Zwiers (2013), Global Increasing Trends in Annual Maximum Daily Precipitation,
796 *Journal of Climate*, 26(11), 3904-3918, doi:10.1175/jcli-d-12-00502.1.

797 Wu, X. (2012), Beijing urban impervious surface space-time pattern analysis and planning applications, Hohhot city.

798 Xu, M., C.-P. Chang, C. Fu, Y. Qi, A. Robock, D. Robinson, and H.-m. Zhang (2006a), Steady decline of east Asian
799 monsoon winds, 1969–2000: Evidence from direct ground measurements of wind speed, *Journal of Geophysical*
800 *Research*, 111(D24), doi:10.1029/2006jd007337.

801 Xu, Y., S. Liu, F. Hu, N. Ma, Y. Wang, Y. Shi, H. Jia (2009) Influence of Beijing urbanization on the characteristics of
802 atmospheric boundary layer. *Chinese Journal of Atmospheric Sciences*, 33(4), 859-867. (in Chinese)

803 Xu, Z. X., L. Zhang, and B. Q. Ruan (2006b), Analysis on the spatio-temporal distribution of precipitation in the Beijing
804 region, *Arid Land Geography*, 29(2), 186-192.

805 Yang, F. L., and K. M. Lau (2004), Trend and variability of China precipitation in spring and summer: Linkage to
806 sea-surface temperatures, *International Journal of Climatology*, 24(13), 1625-1644, doi:10.1002/joc.1094.

807 Yang, G., L. C. Bowling, K. A. Cherkauer, and B. C. Pijanowski (2011), The impact of urban development on hydrologic
808 regime from catchment to basin scales, *Landscape and Urban Planning*, 103(2), 237-247,
809 doi:10.1016/j.landurbplan.2011.08.003.

810 Yang, L., F. Tian, J. A. Smith, and H. Hu (2014), Urban signatures in the spatial clustering of summer heavy rainfall
811 events over the Beijing metropolitan region, *Journal of Geophysical Research: Atmospheres*, 119(3), 1203-1217,
812 doi:10.1002/2013JD020762.

813 Yang, P., G. Ren, W. Hou, and W. Liu (2013), Spatial and diurnal characteristics of summer rainfall over Beijing
814 Municipality based on a high-density AWS dataset, *Int. J. Climatol.*, 33(13), 2769-2780, doi:10.1002/joc.3622.

815 Yin, S., W. Li, D. Chen, J.-H. Jeong, and W. Guo (2011), Diurnal variations of summer precipitation in the Beijing area
816 and the possible effect of topography and urbanization, *Advances in Atmospheric Sciences*, 28(4), 725-734,
817 doi:10.1007/s00376-010-9240-y.

- 818 You, H., W. Liu, and G. Ren (2014), Variation characteristics of precipitation extremes in Beijing during 1981-2010,
819 *Climatic and Environmental Research*, 19(1), 69-77, doi:10.3878/j.issn.1006-9585.2012.12143.
- 820 Zawilski, M., and A. Brzezińska (2013), Areal rainfall intensity distribution over an urban area and its effect on a
821 combined sewerage system, *Urban Water Journal*, 1-11, doi:10.1080/1573062x.2013.831909.
- 822 Zhai, P., X. Zhang, H. Wan, and X. Pan (2005), Trends in Total Precipitation and Frequency of Daily Precipitation
823 Extremes over China, *Journal of Climate*, 18(7), 1096-1108, doi:10.1175/jcli-3318.1.
- 824 Zhai, Y., Y. Guo, J. Zhou, N. Guo, J. Wang, and Y. Teng (2014), The spatio-temporal variability of annual precipitation
825 and its local impact factors during 1724-2010 in Beijing, China, *Hydrological Processes*, 28(4), 2192-2201,
826 doi:10.1002/hyp.9772.
- 827 Zhang, C., C. Ji, Y. Kuo, S. Fan, C. Xuan, and M. Chen (2005), Numerical simulation of topography effects on the “00.7”
828 server rainfall in Beijing, *Progress in Natural Science*, 15(9), 818-826, doi:10.1080/10020070512331342970.
- 829 Zhang, C. L., F. Chen, S. G. Miao, Q. C. Li, X. A. Xia, and C. Y. Xuan (2009), Impacts of urban expansion and future
830 green planting on summer precipitation in the Beijing metropolitan area, *J. Geophys. Res.-Atmos.*, 114, 26,
831 doi:10.1029/2008jd010328.
- 832 Zhang, D.-L., Y. Lin, P. Zhao, X. Yu, S. Wang, H. Kang, and Y. Ding (2013a), The Beijing extreme rainfall of 21 July
833 2012: “Right results” but for wrong reasons, *Geophys. Res. Lett.*, 40(7), 1426-1431, doi:10.1002/grl.50304.
- 834 Zhang, J., and H. You (2013), Study on Changes of Precipitation Extremes in Beijing, *Climate Change Research Letters*,
835 02(04), 131-136, doi:10.12677/ccrl.2013.24022.
- 836 Zhang, Q., V. P. Singh, J. Li, and X. Chen (2011), Analysis of the periods of maximum consecutive wet days in China. *J.*
837 *Geophys. Res.*, 116, D23106, doi:10.1029/2011JD016088.
- 838 Zhang, Q., V. P. Singh, J. Peng, Y. D. Chen, and J. Li (2012), Spatial-temporal changes of precipitation structure across
839 the Pearl River basin, China, *Journal of Hydrology*, 440-441, 113-122, doi:10.1016/j.jhydrol.2012.03.037.
- 840 Zhang, X., H. Wan, F. W. Zwiers, G. C. Hegerl, and S.-K. Min (2013b), Attributing intensification of precipitation
841 extremes to human influence, *Geophys. Res. Lett.*, 40(19), 5252-5257, doi:10.1002/grl.51010.
- 842 Zhang, Y., J. A. Smith, L. Luo, Z. Wang, and M. L. Baeck (2014), Urbanization and rainfall variability in the Beijing
843 metropolitan region, *Journal of Hydrometeorology*, in press, doi: 10.1175/JHM-D-13-0180.1
- 844 Zheng, S. Y., and S. H. Liu (2008), Urbanization effect on climate in Beijing, *Climatic and Environmental Research*,
845 13(2), 123-133.
- 846 Zheng, Z., Z. Wang, and H. Gao (2013), Characteristics of extreme precipitation events in summer and its effect on
847 urbanization in Beijing area, *Meteorological Monthly*, 39(12), 1635-1641, doi:10.7519/j.issn.1000-0526.2013.12.012.
- 848 Zhong, Y., Y. Jia, and Z. Li (2013), Spatial and temporal changes of maximum 1h precipitation intensity in Beijing region
849 in last 53 years, *Journal of China Hydrology*, 33(1), 32-37.
- 850 Zhu, L., Y. Chen, R. Yan, T. Shen, L. Jiang, and Y. Wang (2012), Characteristics of precipitation and temperature changes

851 in Beijing city during 1951-2010, *Resource Science*, 34(7), 1287-1297.

852

853

856 **Figure 1.** The location and topography map of Beijing and the 43 rain gauges in Beijing. Red solid
857 lines denote the boundaries of the six areas. UA, ISAS, ISAN, OSA, NWMA, and SWMA refer to
858 the urban area, inner suburb area in south, inner suburb area in north, outer suburb area, northwestern
859 mountainous area, and southwestern mountainous area, respectively.

860 **Figure 2.** The time series of mean precipitation from 1950-2012 in the Beijing area in (a) spring
861 (March, April, and May), (b) summer (June, July, and August), (c) autumn (September, October and
862 November), (d) winter (December, January and February), (e) warm season (June to September), (f)
863 annual.

864 **Figure 3.** Box plots of the decadal-average precipitation from 1950-2012 in (a) spring, (b) summer,
865 (c) autumn, (d) winter, (e) warm season and (f) annual. The square marks represent the mean value of
866 precipitation data. The top, middle and bottom horizontal line represent the 75th percentile, median
867 and the 25th percentile, respectively. The solid and hollow circles represent the maximum and
868 minimum values.

869 **Figure 4.** M-K test statistic results of the annual mean precipitation and seasonal mean precipitation
870 from 1950-2012: (a) spring, (b) summer, (c) autumn, (d) winter, (e) warm season, (f) annual. Dashed
871 lines are the confidence limits at the 95% confidence level.

872 **Figure 5** (a) Percentage contributions of monthly precipitation to the annual precipitation amount,
873 and (b) annual cycle of mean precipitation for different periods over the Beijing area

874 **Figure 6.** Distribution of decadal-averaged warm-season precipitation (mm) in the Beijing area: (a)
875 from 1980-1989 (1980s), (b) 1990-1999 (1990s), (c) 2000-2009 (2000s), and the differences of
876 precipitation for the three decades: (d) between 1980s and 1990s, (e) between 1990s and 2000s, (f)
877 between 1980s and 2000s.

878 **Figure 7.** Spatial distribution of precipitation trends in the warm season across the Beijing area from
879 1980-2012. Red triangles represent insignificant increasing trend. Green triangles denote
880 insignificant decreasing trend. Green triangles with black circles show significant decreasing trend at
881 the 95% confidence level. D.T. represents a decreasing trend and a U.T. upward trend.

882 **Figure 8.** Time series and Mann-Kendall's test statistics values of the precipitation amount in warm
883 season for different parts of the Beijing area from 1980-2012.

884 **Figure 9.** Spatial variation (a and b) and the M-K-based trends (c and d) of precipitation intensity
885 from 1980-2012. Left panel (a and c) represents the hourly mean precipitation intensity, and right
886 panel (b, d) is the maximum 1hr precipitation intensity. PI indicates precipitation intensity.

887 **Figure 10.** Time series and the Mann-Kendall test results of mean hourly precipitation intensity in

888 the warm season for the six areas in the Beijing area during the past three decades

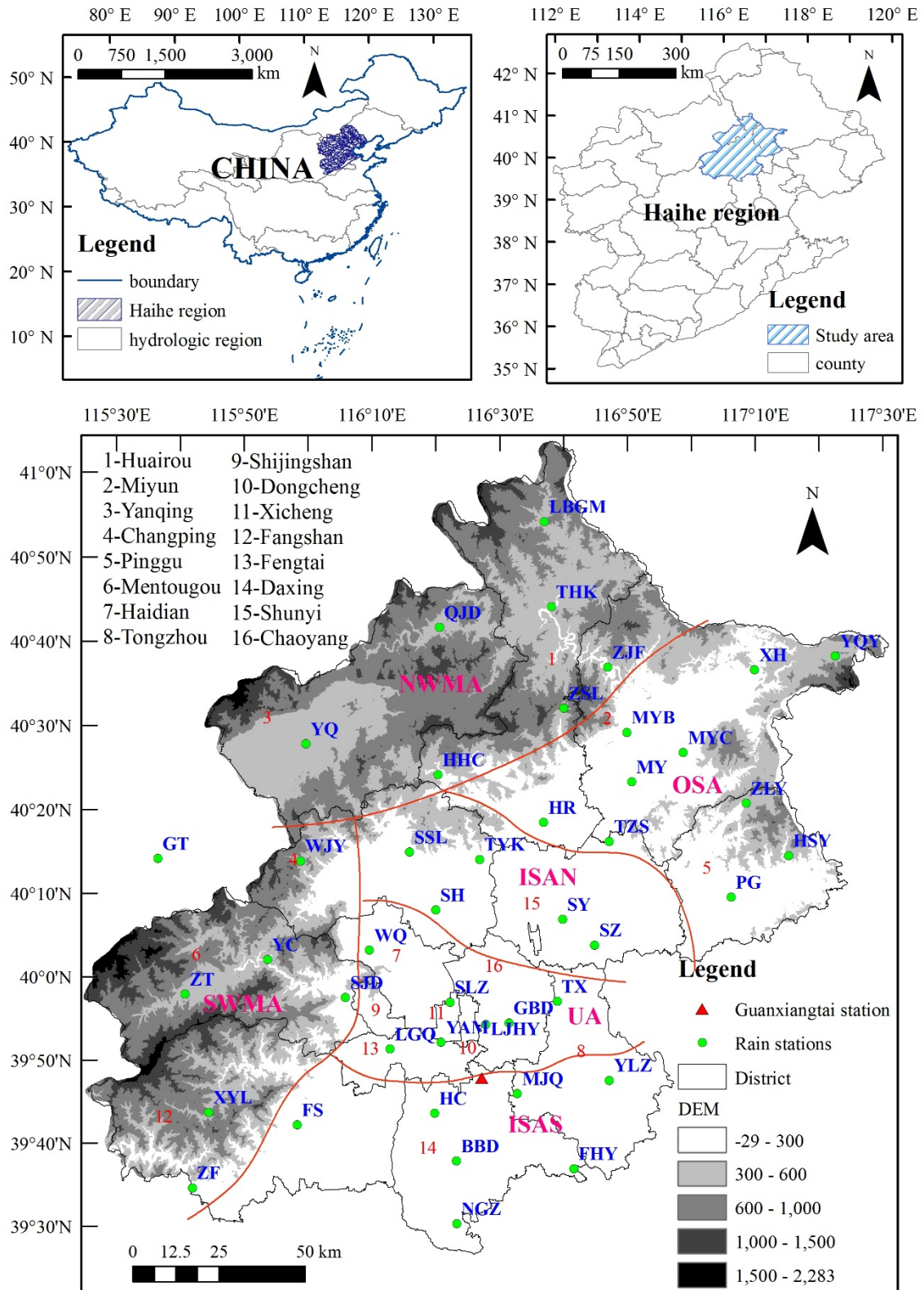
889 **Figure 11.** Time series and the Mann-Kendall test results of maximum 1-hour precipitation intensity
890 in the warm season for the six areas in the Beijing area over the past three decades

891 **Figure 12.** (a) Mean temperature for Beijing Guanxiangtai weather station from 1951-2012, and (b)
892 warm season precipitation and the urban built-up areas in Beijing from 1980-2012. The meaning of
893 the lines with symbols is illustrated in the lower-left of each plot, and the lines without symbols are
894 their corresponding linear tendency change (see linear-fitted equations).

895 **Figure 13.** Variation of surface water availability in the Beijing area: variation of inflow and storage
896 capacity for (a) the Guanting and (b) Miyun reservoirs, and variation of the groundwater table (c) in
897 the plain areas of Beijing and (d) in the districts. CY-Chaoyang, FT-Fengtai, HD-Haidian,
898 SJS-Shijingshan, TZ-Tongzhou, DX-Daxing, FS-Fangshan, MTG-Mengtougou, CP-Changping,
899 SY-Shunyi, YQ-Yanqing, HR-Huairou, MY-Miyun, PG-Pinggu

900 **Figure 14.** (a) Changes of water-use structure from 1980-2012 and (b) changes of water-use structure
901 from 2001-2012.

902 **Table 1.** Information for all the stations and the six regions in the Beijing area



904

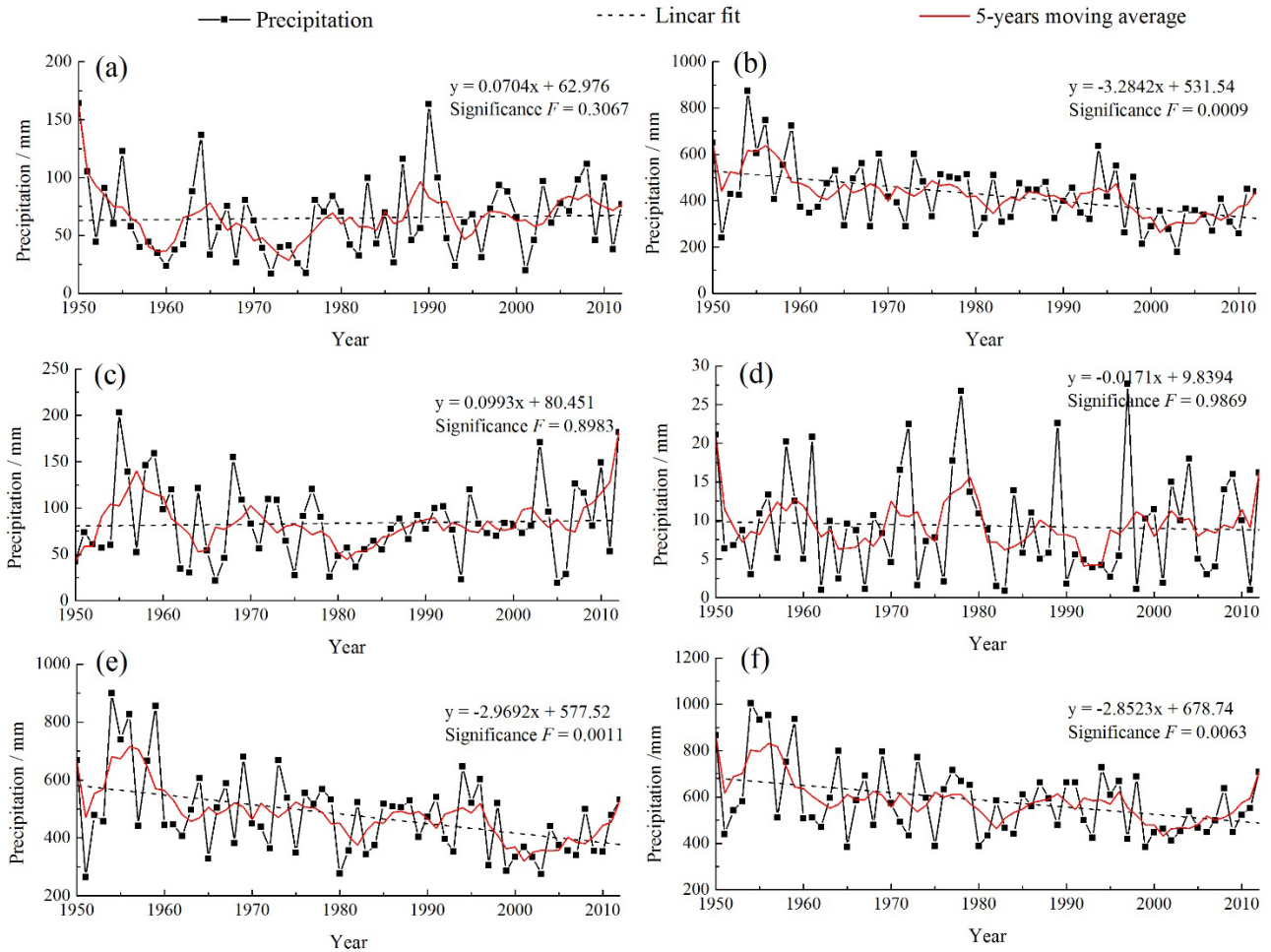
905

906

907

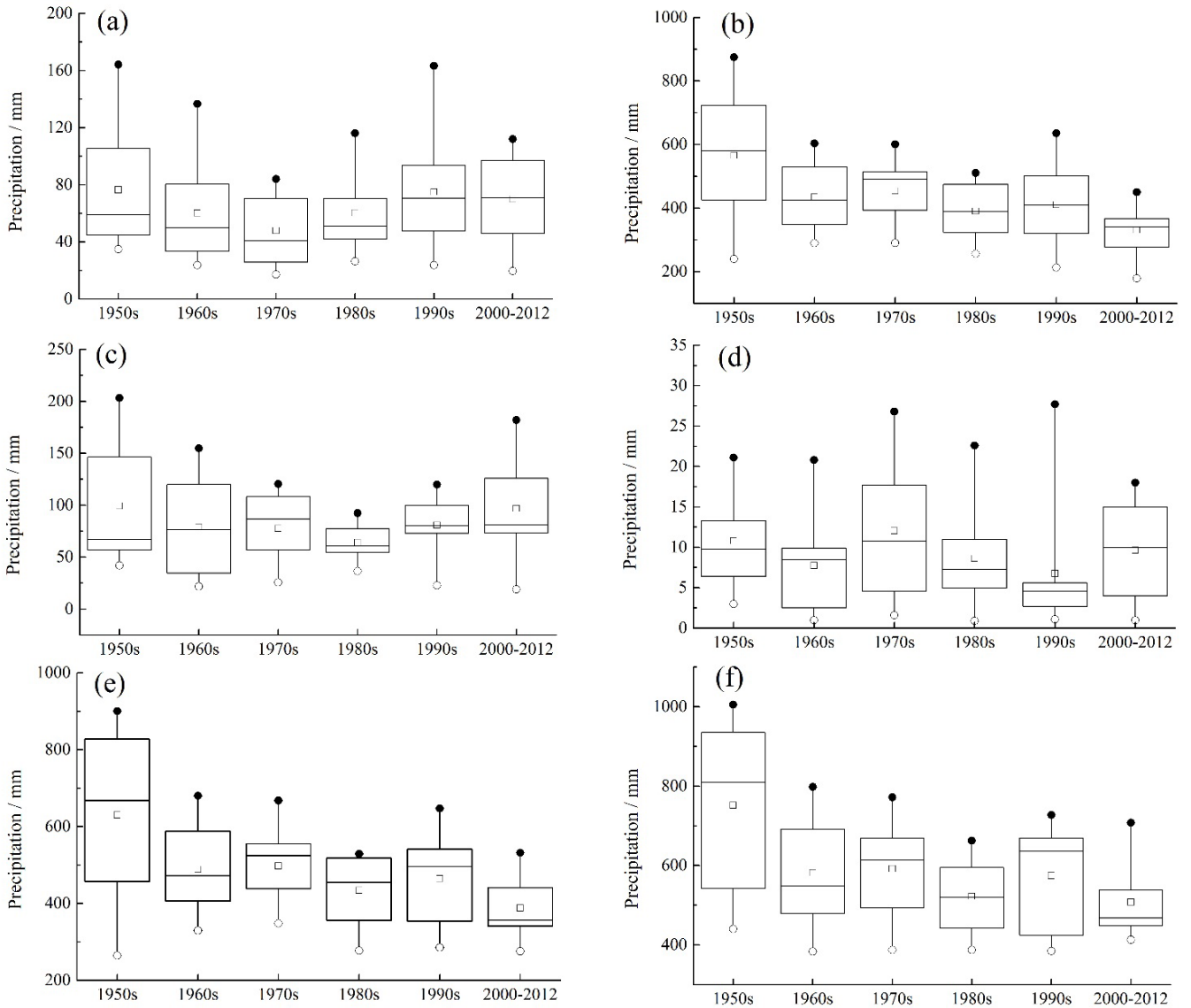
Figure 1. The location and topography map of Beijing and 43 rain gauges in Beijing. Red solid lines denote the boundaries of the six areas. UA, ISAS, ISAN, OSA, NWMA, and SWMA refer to the urban area, inner suburb area in south, inner suburb area in north, outer suburb area, northwestern mountainous area, and southwestern

908 mountainous area.



909

910 Figure 2. The time series of mean precipitation from 1950-2012 in the Beijing area in (a) spring (March, April, and
 911 May), (b) summer (June, July, and August), (c) autumn (September, October and November), (d) winter (December,
 912 January and February), (e) warm season (June to September), (f) annual.



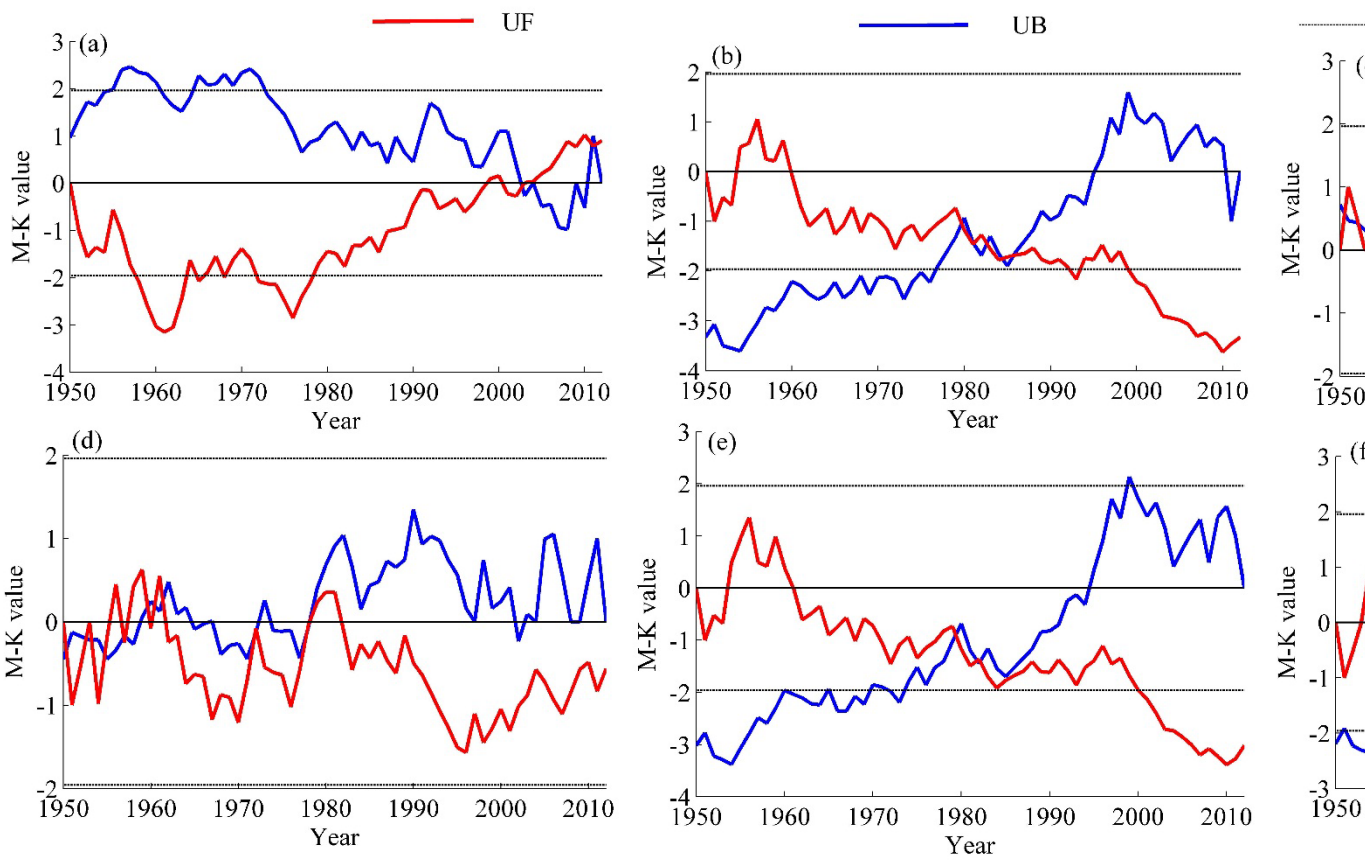
913

914 Figure 3. Box chart of the decadal-average precipitation from 1950-2012 in (a) spring, (b) summer, (c) autumn, (d)

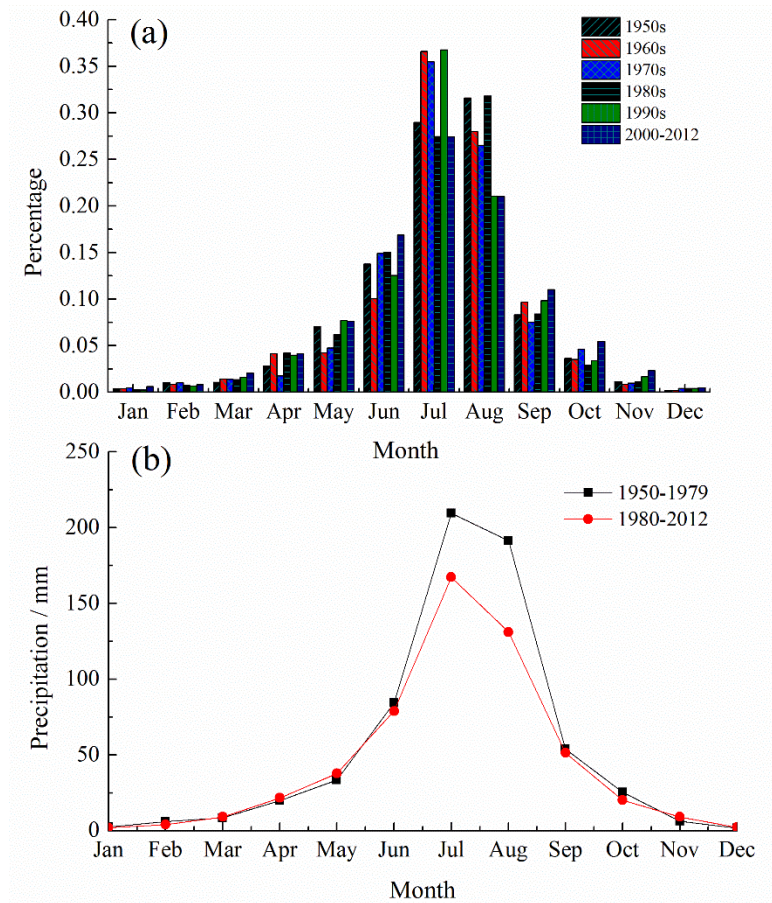
915 winter, (e) warm season and (f) annual. Small squares represent the mean value of precipitation data. The top,

916 middle and bottom horizontal line represent the 75th percentile value, median value and the 25th percentile value.

917 The solid and hollow circle represent the maximum and minimum value respectively.



918
 919 Figure 4. M-K statistical test results of the annual mean precipitation and seasonal mean precipitation from 1950-2012: (a) sp
 920 (e) warm season, (f) annual. Dashed lines are the confidence limits at the 95% confidence level

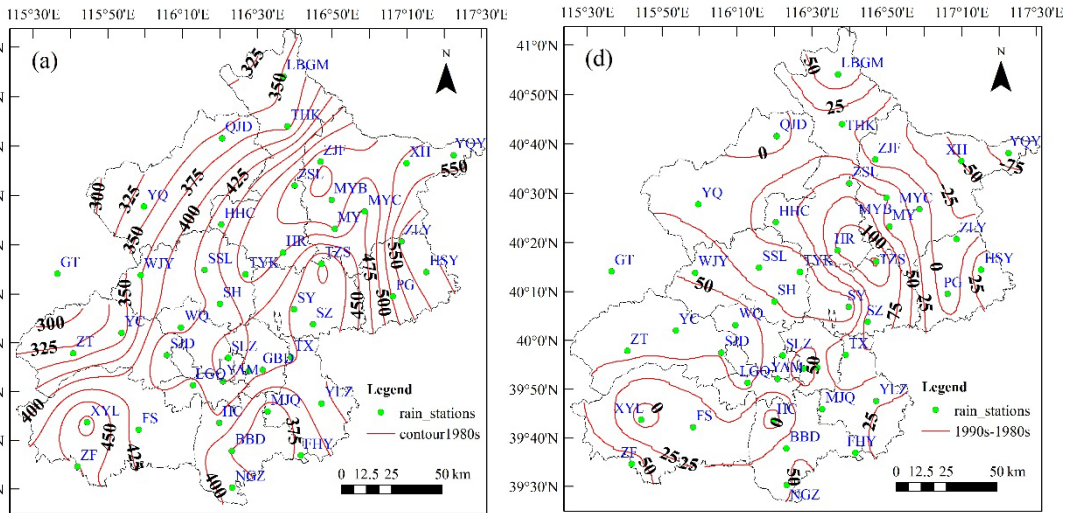


921

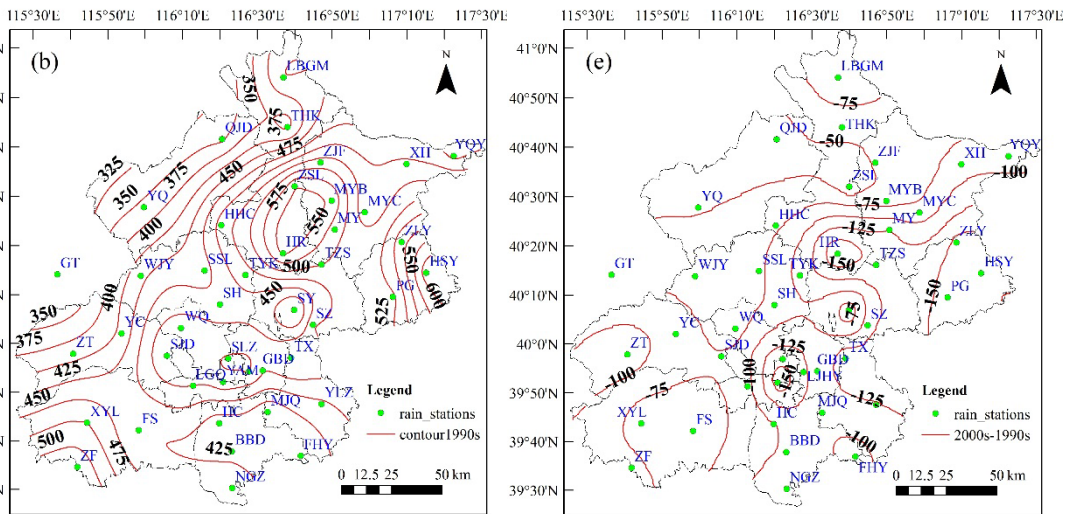
922 Figure 5 (a) Percentage contributions of monthly precipitation to the annual precipitation amount, and (b) annual

923 cycle of mean precipitation for different periods over the Beijing area

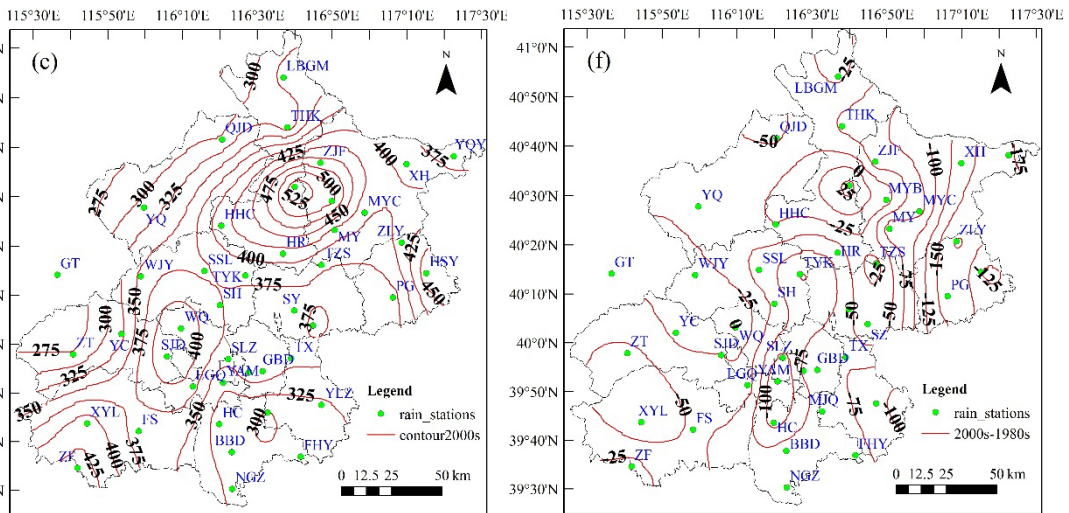
924



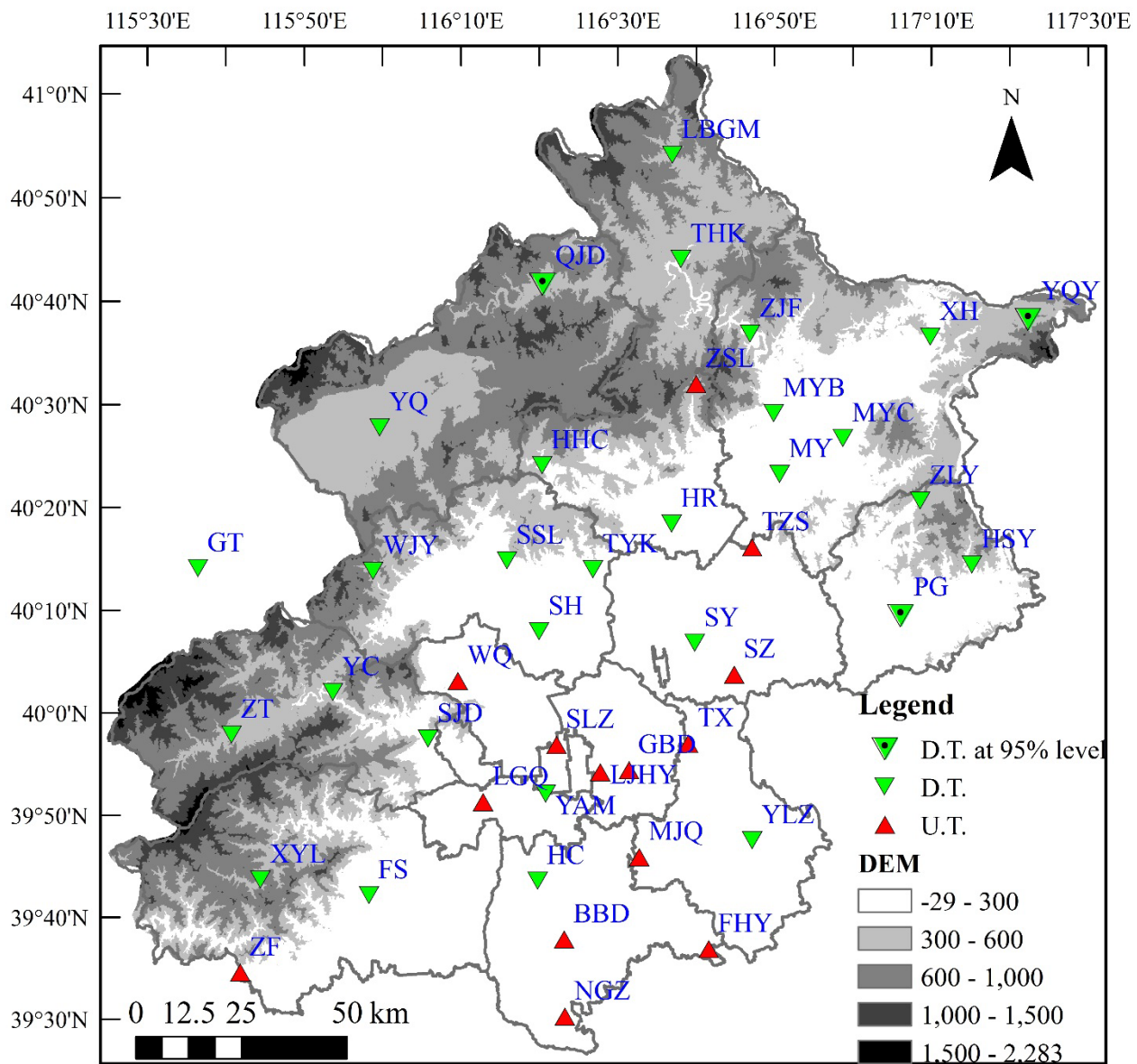
925



926

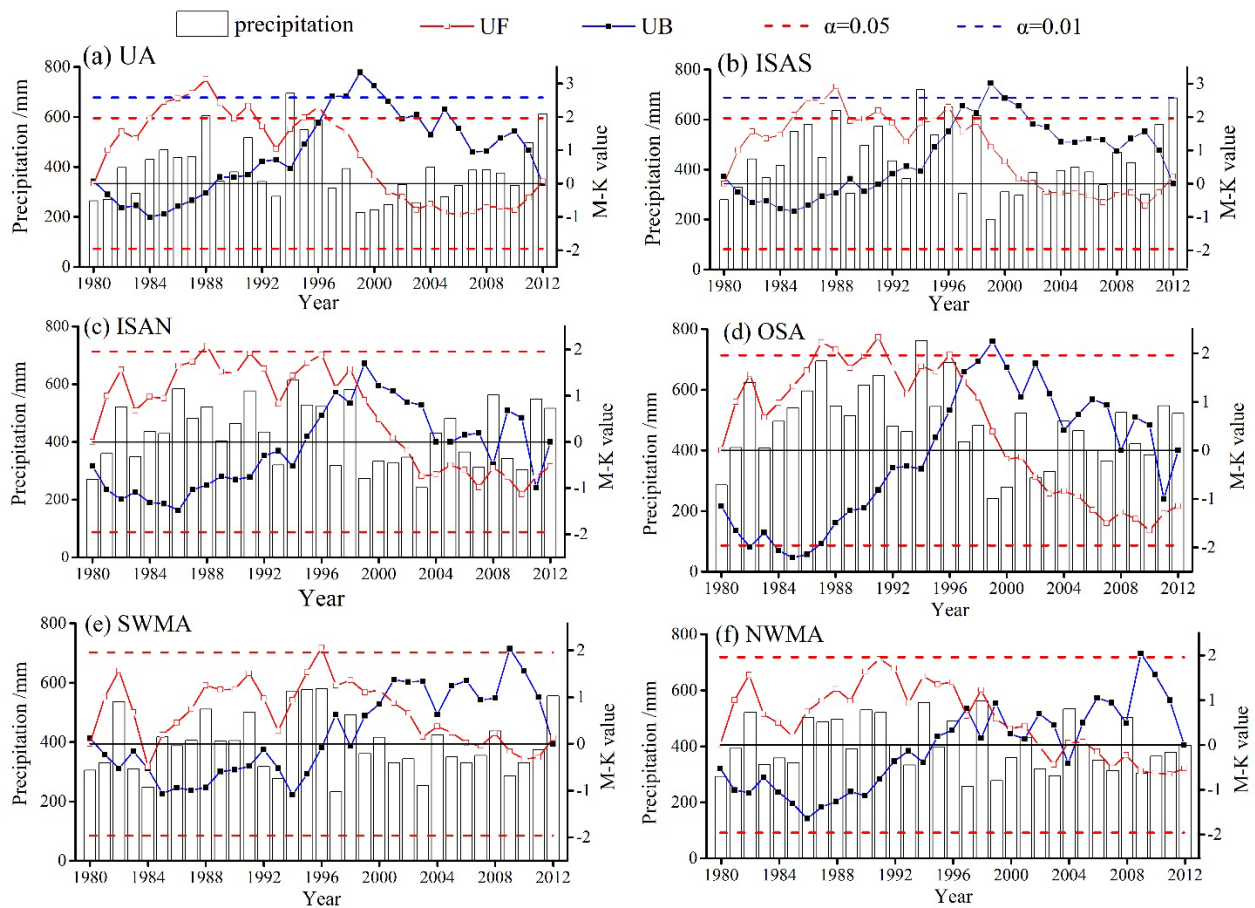


927 Figure 6. Distribution of decadal-averaged warm-season precipitation (mm) in the Beijing area: (a) for 1980-1989
 928 (1980s), (b) 1990-1999 (1990s), (c) 2000-2009 (2000s), and the differences of precipitation for the three decades:
 929 (d) between 1980s and 1990s, (e) between 1990s and 2000s, (f) between 1980s and 2000s.



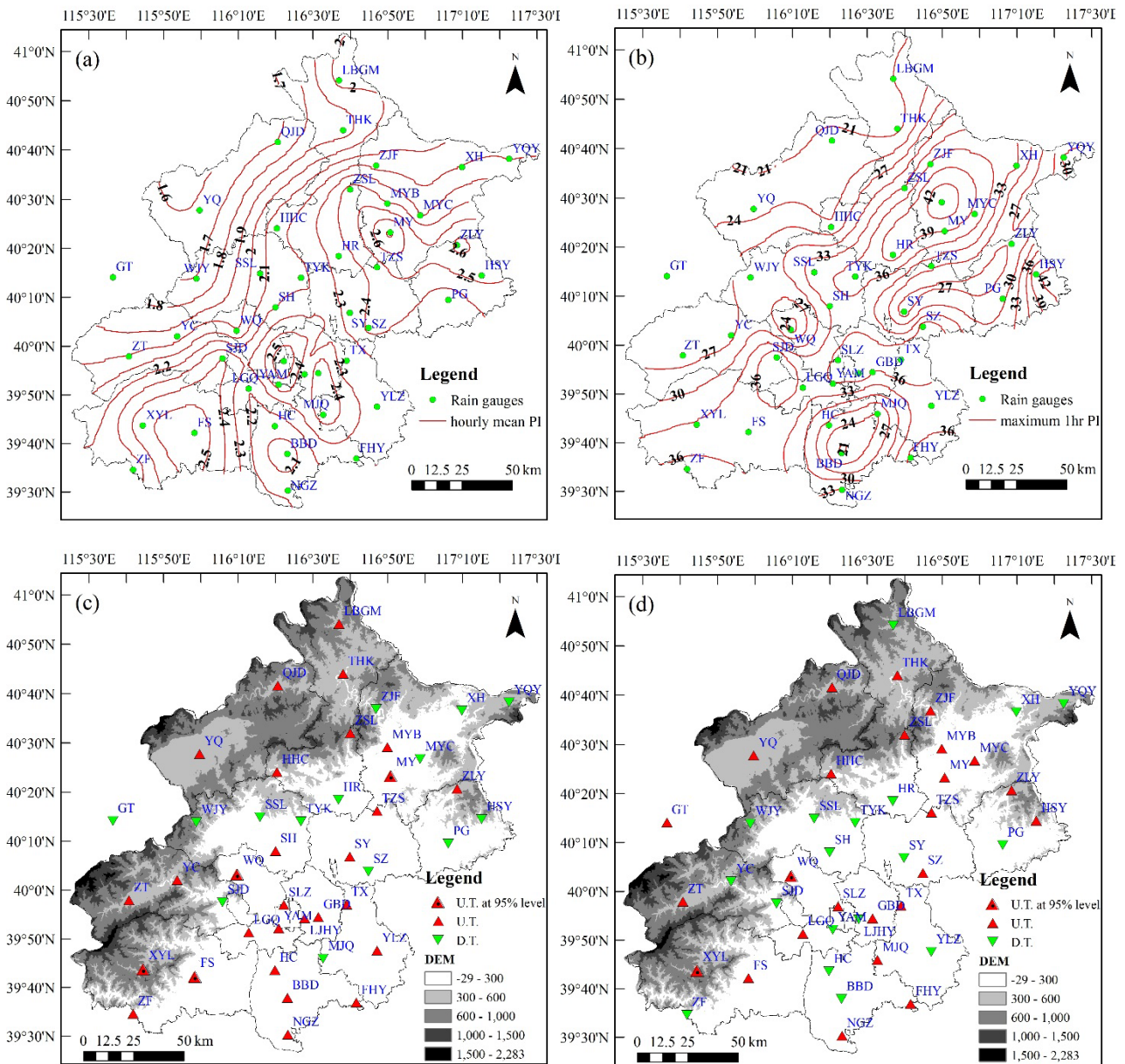
930

931 Figure 7. Spatial distribution of trends of precipitation amount in the warm season across the Beijing area during
 932 1980-2012. Red triangle represents the increasing trends with no significant trends. Green triangle denote
 933 decreasing trends but with no significant trends. Green triangle with black circle show significant decreasing trends
 934 at the 95% confidence level. D.T. represents the decreasing trend and U.T upward trend.



935
936
937

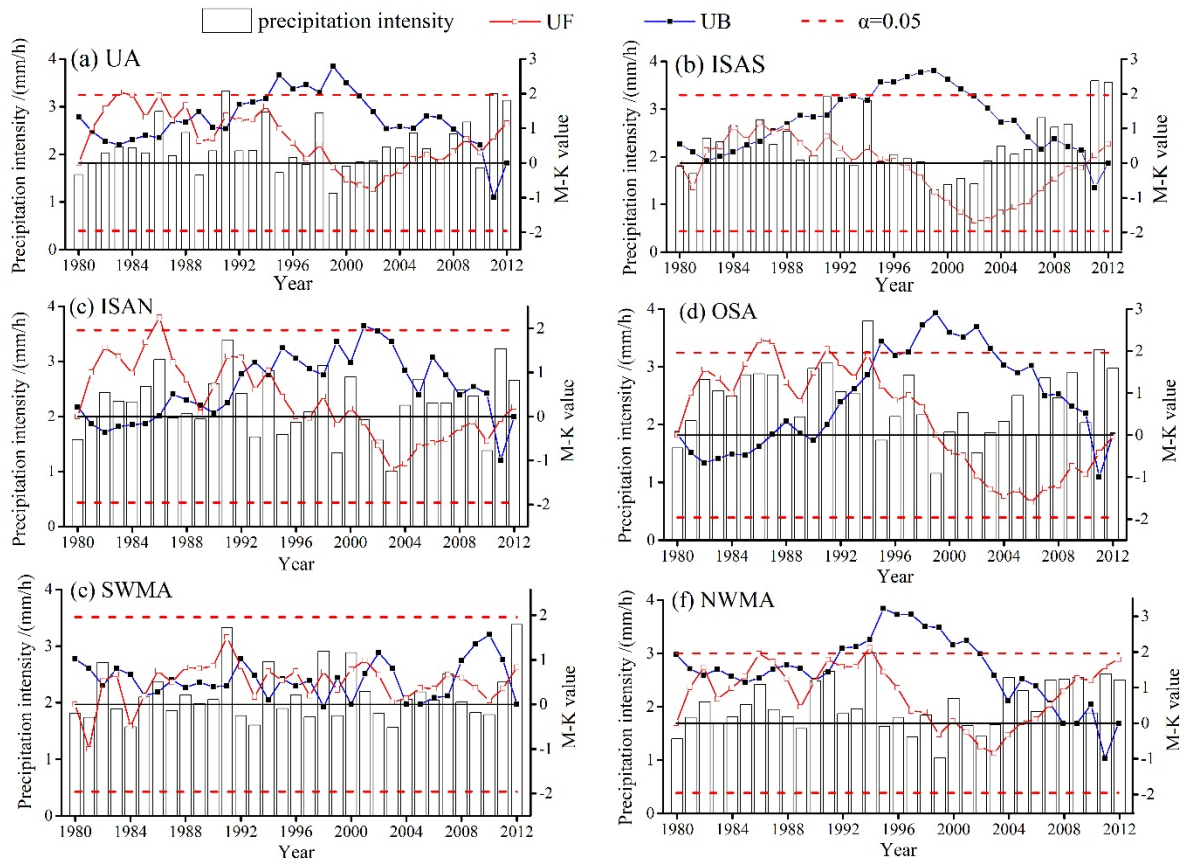
Figure 8. Time series and Mann-Kendall's testing statistics values of the precipitation amount in warm season for different parts of the Beijing area from 1980-2012.



938

939

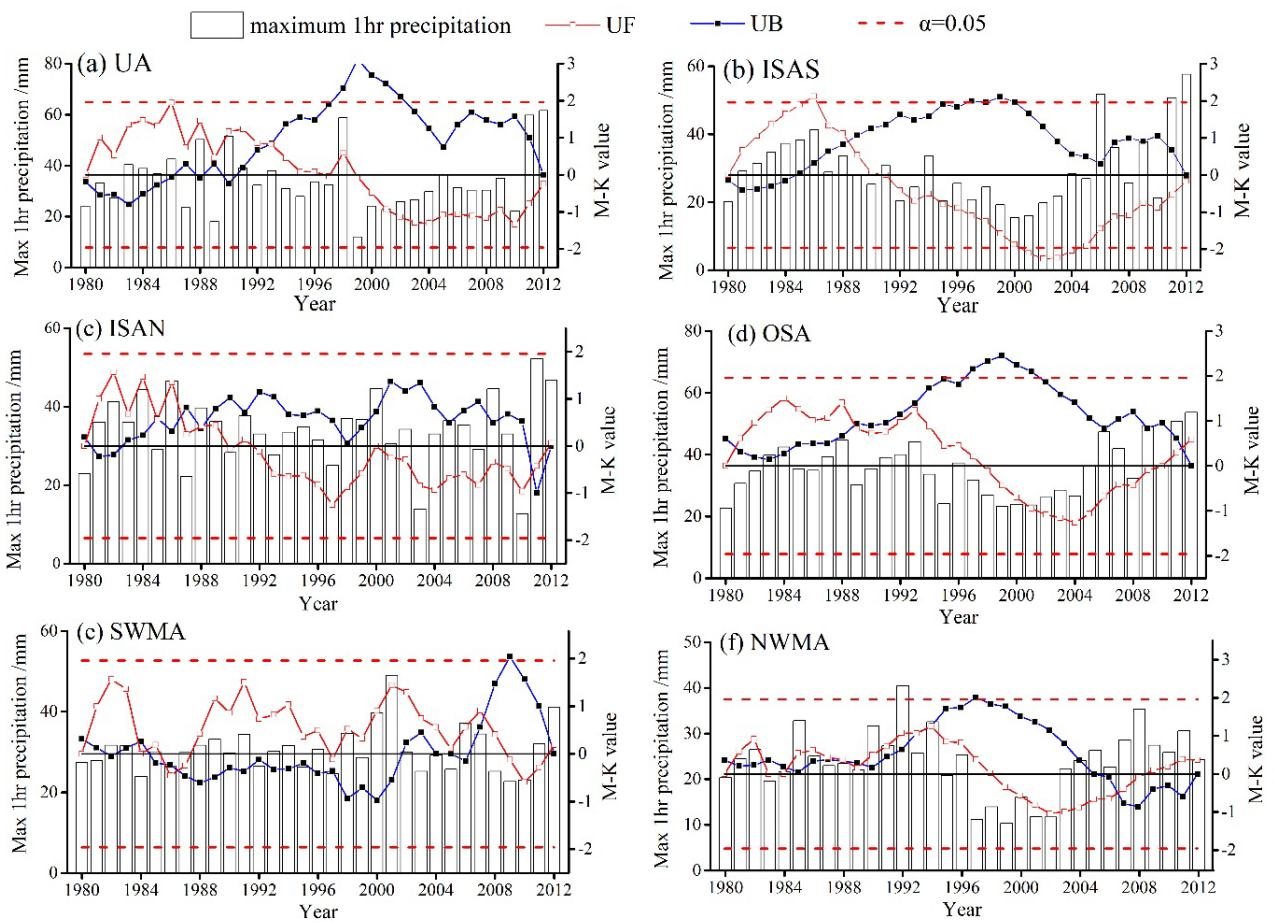
940 Figure 9. Spatial variation (a and b) and M-K trends (c and d) of precipitation intensity during 1980-2012. Left
 941 panel (a and c) represents the hourly mean precipitation intensity, and right panel (b, d) is the maximum 1hr
 942 precipitation intensity. PI means precipitation intensity.



943

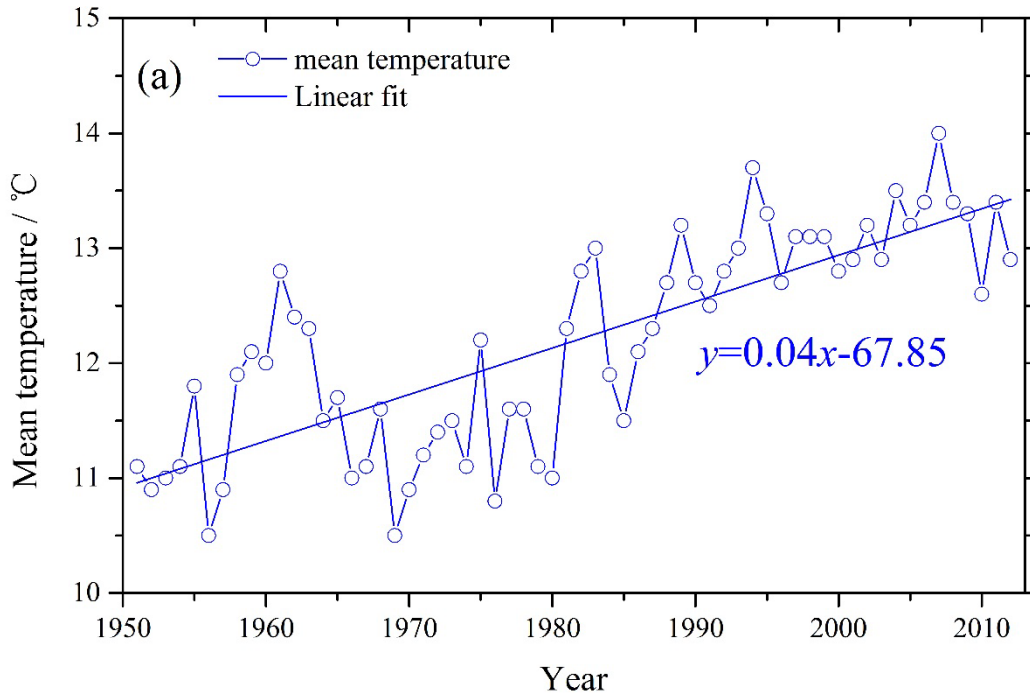
944 Figure 10. Time series and Mann-Kendall results of mean hourly precipitation intensity in the warm season for the

945 six areas in the Beijing area during the past three decades

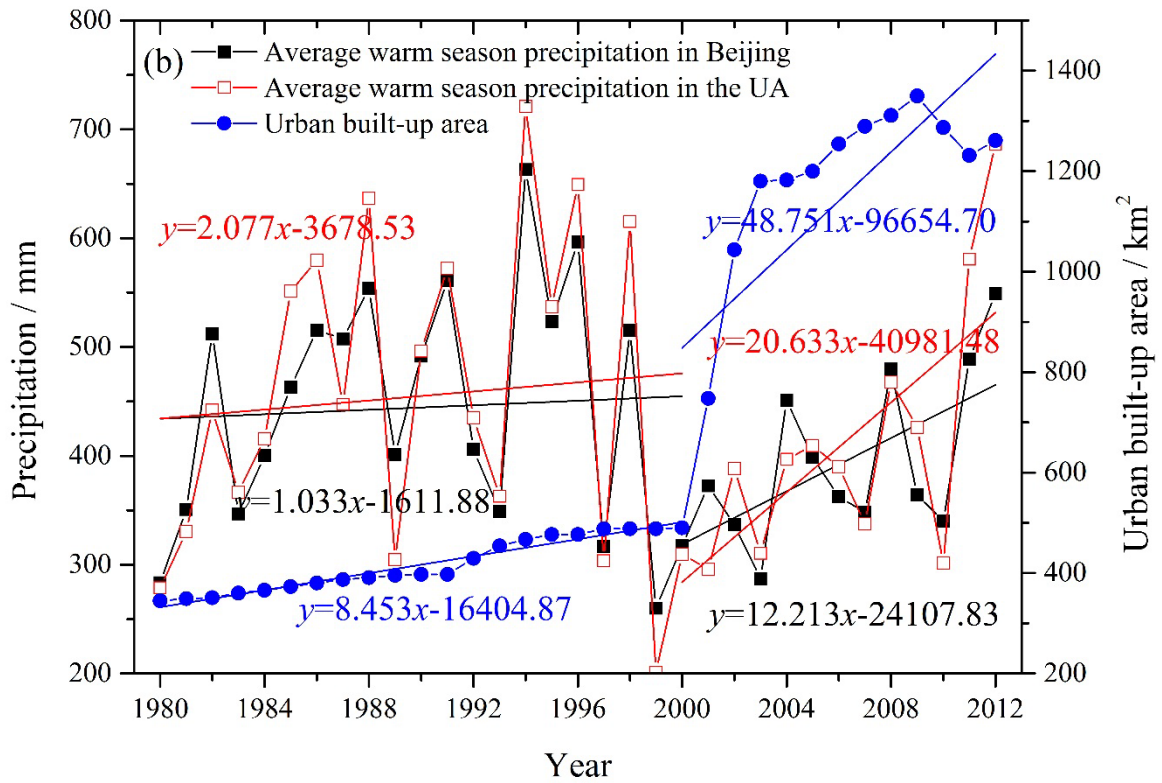


946

947 Figure 11. Time series and Mann-Kendall results of maximum 1-hour precipitation intensity in the warm season for
 948 the six areas in the Beijing area during the past three decades

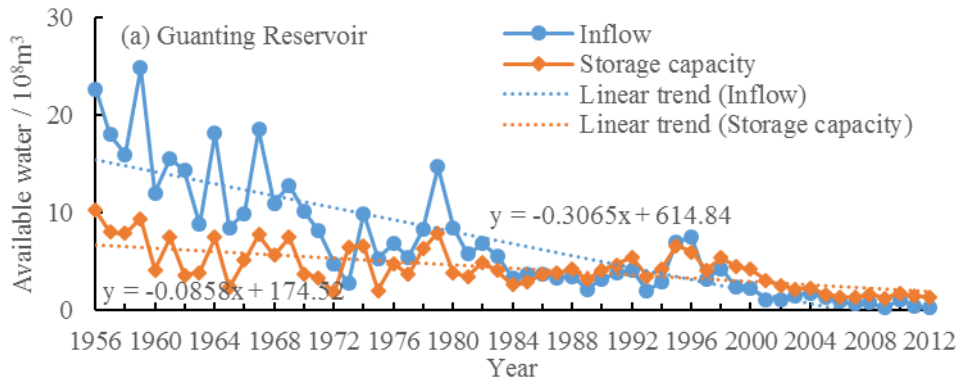


949

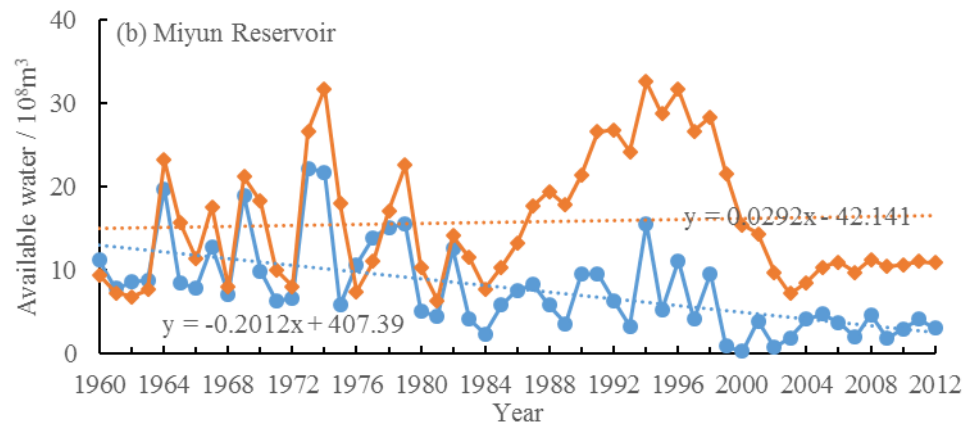


950

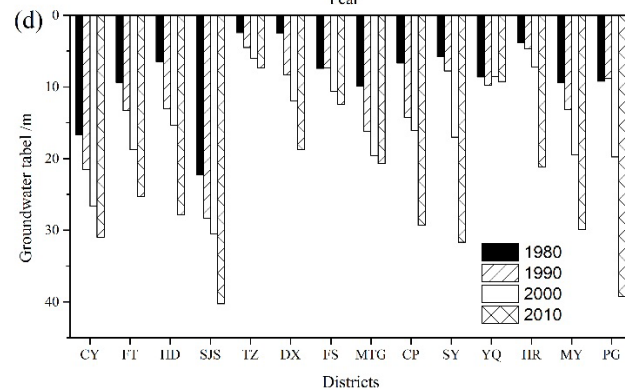
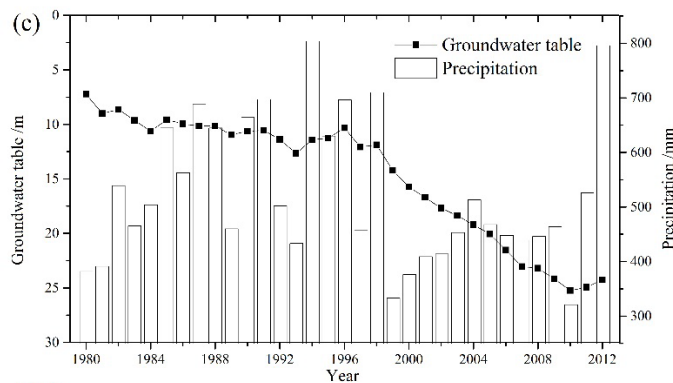
951 Figure 12. (a) Mean temperature for Beijing Guanxiangtai weather station during 1951-2012, and (b) the warm
 952 season precipitation and the urban built-up areas in Beijing during 1980-2012. The meaning of the lines with
 953 symbols is illustrated in the lower-left of each plot, and the lines without symbols are their corresponding linear
 954 tendency change (see linear-fitted equations).



955

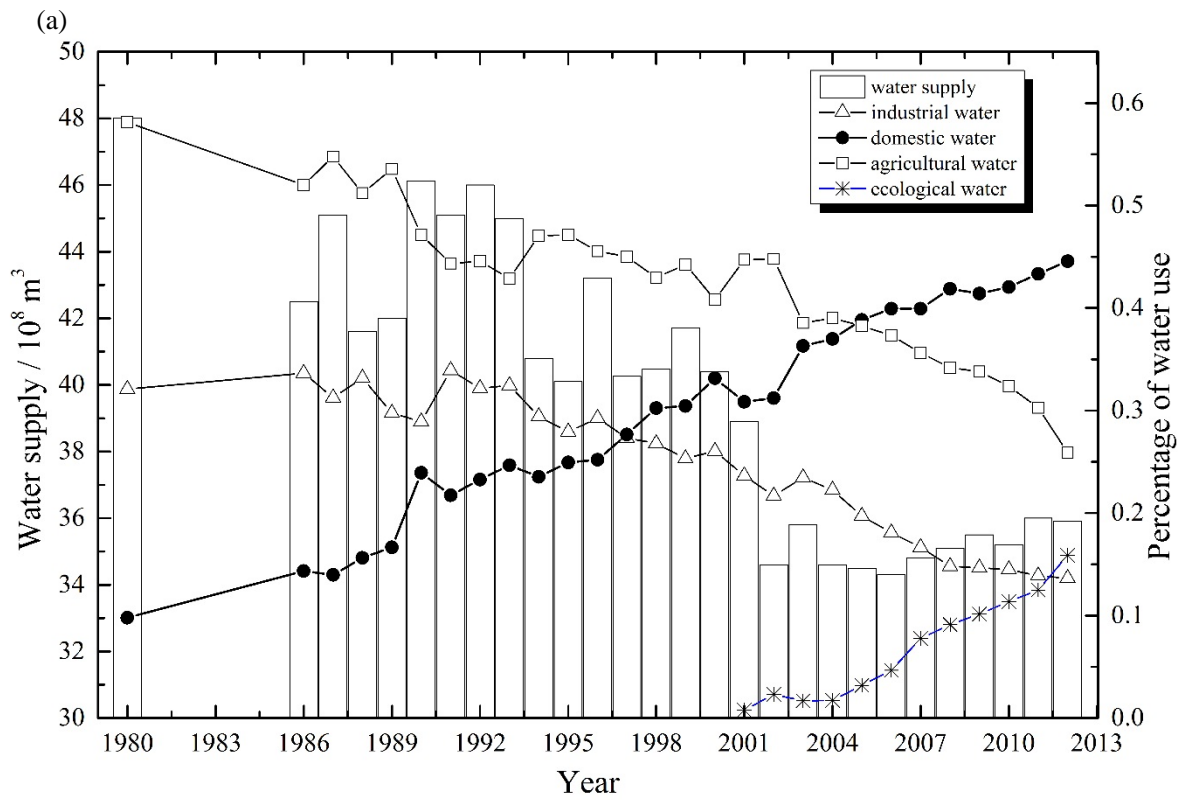


956

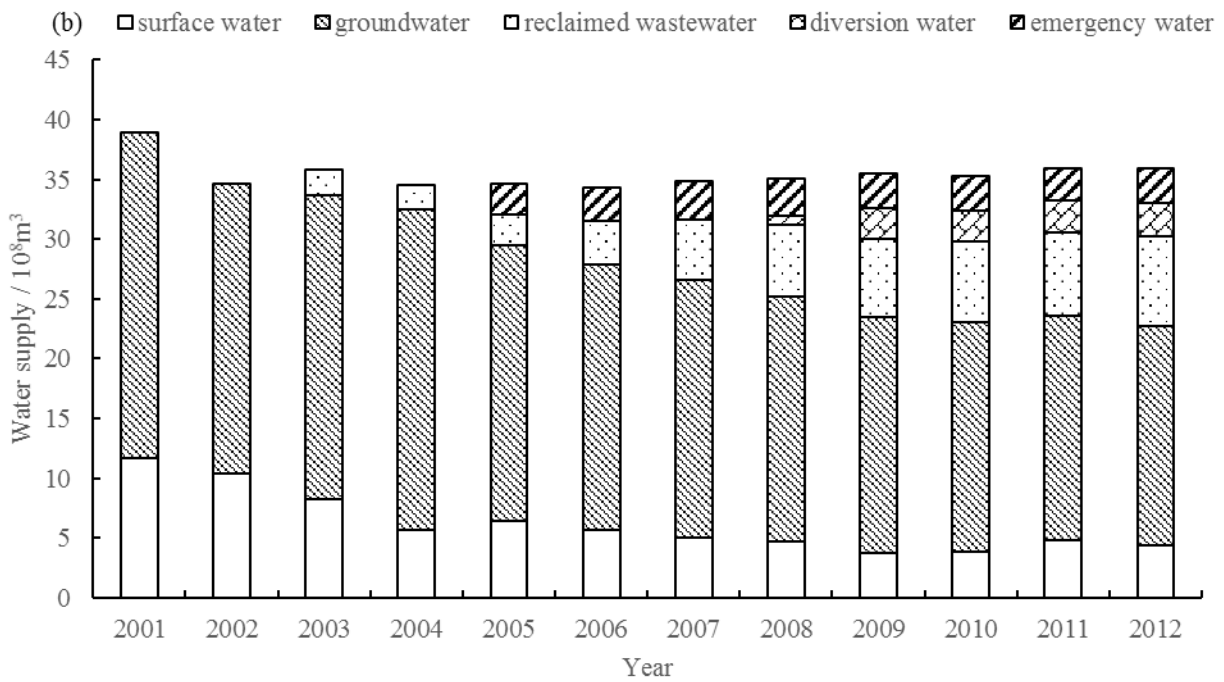


957

958 Figure 13. Variation of surface water availability in the Beijing area: variation of inflow and storage capacity for (a)
 959 the Guanting and (b) Miyun reservoirs, and variation of the groundwater table (c) in the plain areas of Beijing and
 960 (d) in the districts. CY-Chaoyang, FT-Fengtai, HD-Haidian, SJS-Shijingshan, TZ-Tongzhou, DX-Daxing,
 961 FS-Fangshan, MTG-Mengtougou, CP-Changping, SY-Shunyi, YQ-Yanqing, HR-Huairou, MY-Miyun, PG-Pinggu



962



963

964 Figure 14. (a) Changes of water-use structure from 1980-2012 and (b) changes of water-use structure
 965 during 2001-2012.

966 Table 1 Information for all the stations and six regions in the Beijing area

Region	Station Name	Longitude/E	Latitude/N	Elevation / m	Region	Station Name	Longitude/E	Latitude/N	Elevation / m
UA	Songlinzha (SLZ)	116°21'	39°57'	47	ISAS	Majuqiao (MJQ)	116°21'	39°57'	47
	Youanmen (YAM)	116°21'	39°52'	42		Yulinzhuang (YLZ)	116°21'	39°52'	42
	Lejiahuayuan (LJHY)	116°27'	39°54'	37		Fengheying (FHY)	116°27'	39°54'	37
	Gaobeidian (GBD)	116°31'	39°54'	34		Huangcun (HC)	116°31'	39°54'	34
	Wenquan (WQ)	116°10'	40°03'	54		Banbidian (BBD)	116°10'	40°03'	54
	Lugouqiao (LGQ)	116°13'	39°52'	65		Fangshan (FS)	116°13'	39°52'	65
	Tongxian (TX)	116°39'	39°56'	23		Nangezhuang (NGZ)	116°39'	39°56'	23
ISAN	Shunyi (SY)	116°38'	40°07'	39	NWMA	Qianjiadian (QJD)	116°38'	40°07'	39
	Suzhuang (SZ)	116°45'	40°04'	33		Yanqing (YQ)	116°45'	40°04'	33
	Shisanling reservoir (SSL)	116°16'	40°15'	84		Labagoumen (LBGM)	116°16'	40°15'	84
	Shahe (SH)	116°16'	40°07'	39		Tanghekou (THK)	116°16'	40°07'	39
	Taoyukou reservoir (TYK)	116°26'	40°14'	76		Zhangjiafen (ZJF)	116°26'	40°14'	76
OSA	Huangsongyu reservoir (HSY)	117°15'	40°14'	198	SWMA	Huanghuacheng (HHC)	117°15'	40°14'	198
	Pinggu (PG)	117°07'	40°08'	32		Zaoshulin (ZSL)	117°07'	40°08'	32
	Zhenluoying (ZLY)	117°08'	40°20'	276		Zhaitang reservoir (ZT)	117°08'	40°20'	276
	Miyunbai reservoir (MYB)	116°50'	40°28'	98		Yanchi (YC)	116°50'	40°28'	98
	Xiahui (XH)	117°10'	40°37'	198		Sanjiadian (SJD)	117°10'	40°37'	198
	Yaoqiaoyu reservoir (YQY)	117°23'	40°38'	427		Guanting reservoir (GT)	117°23'	40°38'	427
	Miyunchao reservoir (MYC)	116°59'	40°27'	173		Wangjiayuan reservoir (WJY)	116°59'	40°27'	173
	Miyun (MY)	116°51'	40°22'	75		Zhangfang (ZF)	116°51'	40°22'	75
	Huairou reservoir (HR)	116°37'	40°18'	49		Xiayunlin (XYL)	116°37'	40°18'	49
	Tangzhishan (TZS)	116°48'	40°16'	61					